

Spring 1990

# EEG mapping using the personal computer

Zhuan-Zhang Pei

*New Jersey Institute of Technology*

Follow this and additional works at: <https://digitalcommons.njit.edu/theses>



Part of the [Electrical and Electronics Commons](#)

---

## Recommended Citation

Pei, Zhuan-Zhang, "EEG mapping using the personal computer" (1990). *Theses*. 1343.  
<https://digitalcommons.njit.edu/theses/1343>

This Thesis is brought to you for free and open access by the Theses and Dissertations at Digital Commons @ NJIT. It has been accepted for inclusion in Theses by an authorized administrator of Digital Commons @ NJIT. For more information, please contact [digitalcommons@njit.edu](mailto:digitalcommons@njit.edu).

## **Copyright Warning & Restrictions**

The copyright law of the United States (Title 17, United States Code) governs the making of photocopies or other reproductions of copyrighted material.

Under certain conditions specified in the law, libraries and archives are authorized to furnish a photocopy or other reproduction. One of these specified conditions is that the photocopy or reproduction is not to be “used for any purpose other than private study, scholarship, or research.” If a user makes a request for, or later uses, a photocopy or reproduction for purposes in excess of “fair use” that user may be liable for copyright infringement,

This institution reserves the right to refuse to accept a copying order if, in its judgment, fulfillment of the order would involve violation of copyright law.

**Please Note: The author retains the copyright while the New Jersey Institute of Technology reserves the right to distribute this thesis or dissertation**

Printing note: If you do not wish to print this page, then select “Pages from: first page # to: last page #” on the print dialog screen

The Van Houten library has removed some of the personal information and all signatures from the approval page and biographical sketches of theses and dissertations in order to protect the identity of NJIT graduates and faculty.

# EEG Mapping Using The Personal Computer

by  
Zhuan-zhang Pei

Thesis submitted to the Faculty of the Graduate School of the New Jersey  
Institute of Technology in partial fulfillment of the requirements for the  
degree of Master of Science  
1990

# Approval Sheet

**Title of Thesis:** EEG Mapping Using The Personal Computer

**Name of Candidate:** Zhuan-zhang Pei  
Master of Science in Electrical Engineering  
(December, 1989) *May 1990*

**Thesis and Abstract Approved:** \_\_\_\_\_, date \_\_\_\_\_  
Dr. Stanley S. Reisman  
Professor of  
Electrical Engineering

**Signature of other members of the thesis committee** \_\_\_\_\_

\_\_\_\_\_, date \_\_\_\_\_  
Dr. Peter Engler

\_\_\_\_\_, date \_\_\_\_\_  
Dr. Andrew U. Meyer

\_\_\_\_\_, date \_\_\_\_\_

# VITA

NAME: Zhuan-zhang Pei

DEGREE AND DATE TO BE CONFERRED: M.S., 1990

SECONDARY EDUCATION: First Taiguan High School

<u>College attended</u>	<u>Date</u>	<u>Degree</u>	<u>Date of degree</u>
Tianjin Univ.	1981	BSEE	1985
N. J. I. T	1987	MSEE	1990

Major: Electrical Engineering

publications Y. Liu, Y. Mei, Z. Pei " An application of the Improved Minimax Method on the Filter Design" Proceedings of 15th I.C. Conference in Huangshan, Oct. 1985, P.R.C.

Positions held: Research Assistant, N.J.I.T.

## Abstract

Title of Thesis: EEG Mapping Using The Personal Computer

Zhuan-zhang Pei, Master of Science in Electrical Eng.

Thesis directed by: Dr. Stanley S. Reisman.....

An approach for brain electrical activity mapping using a personal computer has been investigated to enhance the visibility of the EEGs. An automatic procedure from data acquisition to the final mapping has been developed for on-line or off-line data processing, in which a table-look-up technique has been introduced to eliminate redundant processing. The power spectra in different EEG frequency bands for four electrodes are coded into 15 colors and mapped on a color monitor. The data correspondings to the areas between electrodes are interpolated by the surface spline method. The mapping speed and smoothness has been optimized. An experiment has been done for 6 subjects, including a normal person, and five patients with different medical histories. The results are mostly in agreement with the pathological reports and can detect some underlying brain dyfunctions which EEG specialists may fail to see. This method may offer an important tool for clinical diagnosis and for future brain study.

# TABLE OF CONTENTS

Abstract .....	I
Acknowledgement .....	II
Chapter 1. Introduction .....	1
Chapter 2. A Review of The EEG .....	7
2.01 Introduction .....	7
2.02 Electroencephalogram .....	8
2.03 Clinical Measurement of The EEG .....	12
Chapter 3. An A/D Convertor .....	15
3.01 Introduction .....	15
3.02 Hardware Configuration .....	16
3.03 Software Program .....	17
Chapter 4. Digital Signal Processing .....	21
4.01 Introduction .....	21
4.02 The Direct DFT Computation .....	22
4.03 Fast Fourier Transform .....	24
Chapter 5. CRT Controller in The PC .....	30
5.01 Introduction .....	30



5.02 CGA .....	33
5.03 EGA .....	37
5.04 Discussion .....	40
Chapter 6. Topographic Mapping Techniques .....	43
6.01 Introduction .....	43
6.02 A Linear Interpolation Method .....	44
6.03 4-Nearest Neighbors Method .....	46
6.04 Surface Spline Method .....	46
6.05 Discussion .....	49
Chapter 7. Experiments and Results .....	51
7.01 Subjects and Methods .....	51
7.02 Results .....	53
7.03 Discussion .....	56
APPENDIX A .....	65
APPENDIX B .....	68
APPENDIX C .....	71
REFERENCES .....	75

## Acknowledgement

I would like to express my gratitude to Dr. Arthur. Winter, M.D., director of N.J.N.I. and Dr. Stanley. S. Reisman, professor, associate chairman of electrical eng. dept. of N.J.I.T., whose guidance, help and encouragement makes it possible to complete this project. I would like to acknowledge the suggestion and help extended by Dr. Peter. Engler in electrical engineering dept. of N.J.I.T. I would like to thank Dr. Andrew. U. Meyer in electrical eng. dept. of N.J.I.T. for serving as a member of my committee. Special thanks to Dr. A. Winter's secretaries and technicians, and Mr. A. Gikas for participating in collecting data. My acknowledgement must also be extended to Dr. D. Stickler in math department of N.J.I.T, who has discussed mathematical problems with me, and Dr. C. Wang in CIS dept. of N.J.I.T., who has given some suggestions on my computer problems. I would like to express my appreciation to my friends, who have provided some information.

# Chapter 1

## Introduction

The electrical activity of the brain in unanesthetized animals was described qualitatively in the nineteenth century, but it was first analyzed in a systematic manner by the German psychiatrist Hans Berger, who introduced the term “electroencephalogram (EEG)” to denote the potential fluctuations recorded from the brain [6]. The recorded potentials are represented by many fluctuating waves, whose frequencies may vary from 1 to 30 Hz.

The EEG has long been a very useful and valuable tool in the clinical diagnosis of brain diseases such as epilepsy because the normal patterns are altered over the brain areas that are diseased or damaged [8]. Usually the evaluation of a patient’s EEG includes visual scanning of the EEG record-

ings by an experienced electroencephalographer (EEG<sub>er</sub>) for the detectable parameters of the wave forms such as spikes, sharpness, slope, duration and amplitude [1]. This process may be time-consuming, especially in the case of long recordings. In addition, disagreement among readers of the same record is possible due to the subjective nature of the analysis. Thus the difficulties inherent in extracting clinically useful information by visual inspection alone from the massive amounts of data contained in multichannel polygraphic recordings have placed limits on the accuracy and range of utility of the electroencephalograph.

Recently several attempts have been made to increase the visibility of the brain electrical activity through computer-based methods in order to circumvent the above-mentioned shortcomings of the visual analysis. In the paper by F. H. Duffy, et al.[4], EEG data are presented which were recorded from multiple scalp electrodes and graphically displayed on a computer-driven color -video screen. This technique is called brain electrical activity mapping (BEAM). The data by Duffy, et al. were processed on a PDP-12 computer with SIGSYS-12 biomedical software, which resulted in mapping of the spectral energy in any individual EEG band. For each map, scalp areas around electrodes are interpolated by the linear three dimensional interpolation method [4]. In the paper by J. E. Desmedt [3], data processing is on a

PDP-11, the somatosensory evoked potentials (SEP) are mapped on a color hardcopying machine, which is specially designed for this mapping purpose. The data associated with the areas around the electrodes are interpolated by the 4-nearest-neighbor interpolation method. In the paper by F. Perrin [2], scalp current density is studied, and is mapped by means of the surface spline interpolation method. These attempts have met with some success. However, most of these systems are equipped quite specifically and at high cost. In addition, some of these methods improve the mapping speed while the scalp surface distribution becomes less smooth. Others have a smoother distribution at the expense of the computational time.

In this project, we use the personal computer with an add-in A/D converter to enhance the visibility of the EEG data contained in the recordings from multiple scalp electrodes. A data acquisition and digital signal processing program have been developed. The spectral energy in EEG bands is displayed on a color monitor and/or printed in a color hardcopy. The areas around electrodes are interpolated by the surface spline interpolation method. The mapping speed, signal processing speed and distribution smoothness have been optimized. The approach is shown in Fig-1.

A four-channel EEG polygraph with four inputs/outputs and four pre-amplifiers is used to record the signals from the scalp electrodes. This four-

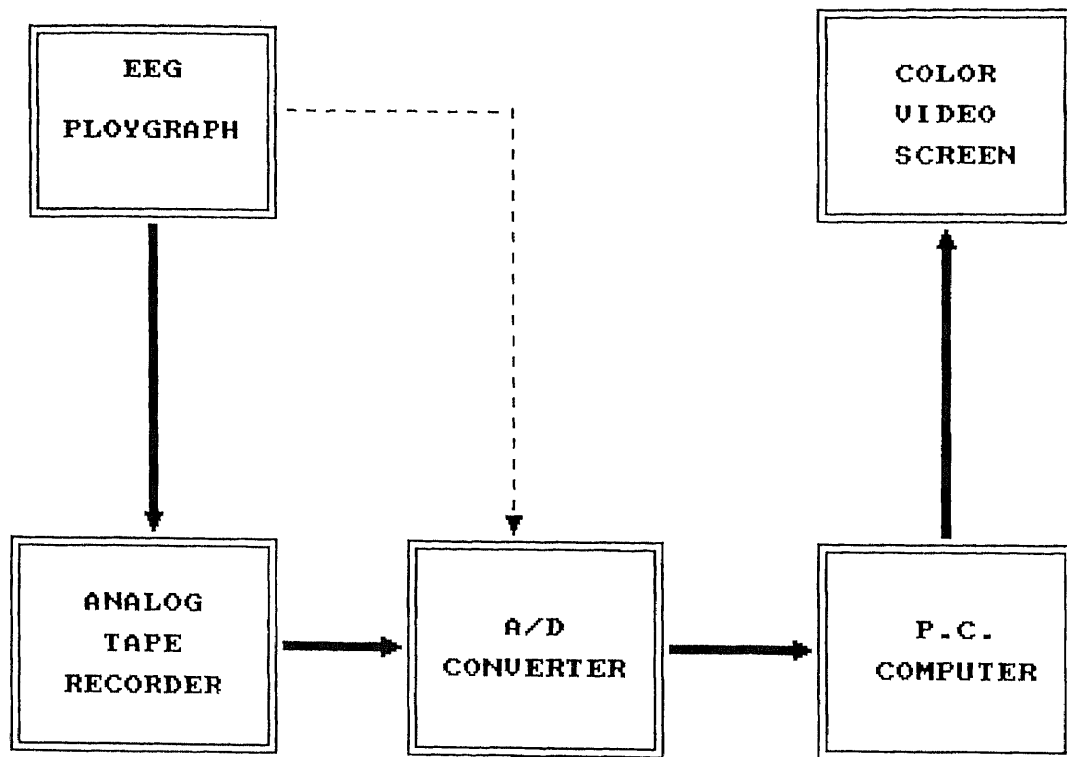


*Fig-1. A block diagram for EEG mapping*

channel signal is input into a computer via an A/D converter for on-line processing or recorded onto audio tape for off-line processing by means of an analog instrumentation tape recorder.

The A/D converter used in this project is the Metrabyte DASH-16, which is a single board with 16 single ended/8 differential analog input channels. It is used to perform control and data acquisition for the PC/XT/AT and compatible computers. The DASH-16 has some powerful features supported by the "DASH16.BIN" subroutine. This subroutine can be used by a BASIC CALL statement. In this project, the data acquisition program is written in BASIC, and the powerful features of the DASH-16 are exploited.

The EEG signals input into the computer are processed by a Fast Fourier Transform (FFT) program. Chapter 4 will be devoted to a discussion of this special algorithm that implements the Discrete Fourier Transform (DFT) with considerable savings in computing time. It is obvious that the development of this FFT algorithm represents the major step in the realization of high-speed real time data processing. In this project, we developed a radix-2 FFT program for four-channel Fourier transforms. Also, a table look-up technique is introduced to increase the speed for the multi-channel Fourier transform.

The next part of the project concerns the display of a map of the EEG information. It is known that the color video screen is controlled by the video board in the computer. The Color Graphics Adapter (CGA) is the video board in most IBM PC/XT or compatible computers and the Enhanced Graphics Adapter (EGA) is the video board in most IBM PC/AT or compatible computers. Their major functions are performed by their CRT controllers to control the resolutions and attributes of the video screen. In this project, we have programmed the CGA/EGA to create a new mode for mapping purposes with  $80 \times 100$  resolution in 16 different colors. We also developed a new plotting subroutine for this new mode.

A topographic map of the head region is formed by a  $60 \times 60$  matrix.

This results in 3600 pixels in two dimensions. The positions of the four electrodes are selected as  $F_z$ ,  $C_3$ ,  $C_4$  and  $P_z$ , based on the international standard 10-20 system (see figure 3). The areas between electrodes are interpolated smoothly by the first degree surface spline interpolation method, which will be described more fully in chapter 6.

The experimental data have been acquired from six subjects, a normal person, and five patients with pathologically different medical histories, this aspect will be fully discussed in Chapter 7.



# Chapter 2

## A Review of EEG

### 2.0.1 Introduction

A normal person's state of consciousness, i.e., whether awake, asleep, drowsy, etc., is defined as the pattern of the brain activity that can be recorded electrically, usually as the electric-potential difference between two points on the scalp (conceptual EEG) [5]. Thus the EEG is an important tool in identifying the different conscious states. For an abnormal person, this normal EEG patterns are altered over brain areas that are diseased or damaged. For example, a common neurological disease associated with distinctive, abnormal EEG patterns is epilepsy. Thus the EEG is a useful clinical tool for diagnosis

of brain defects. We will now review some basic concepts of the EEG

## 2.0.2 Electroencephalogram

Electrical recordings from the exposed surface of the brain or from the outer surface of the head demonstrate continuous oscillating electrical activity within the brain. Both the intensity and patterns of this electrical activity are determined to a great extent by the overall excitation of the brain resulting from functions in the reticular activating system. The undulations in the recorded electrical potentials are called brain waves and the entire record is called an electroencephalogram (EEG) [6].

The EEG patterns are the result of varying extracellular current flows in the patch of cerebral cortex which underlines the recording electrode, the current flows reflecting varying degrees of activity of the individual cortical neurons [7]. While we usually think of neuronal activity in terms of action potentials, action potentials contribute little to the EEG except in unusual circumstance when the activity in a large group of neurons is synchronized. The EEG is largely due to summed postsynaptic potentials, particularly in the large neurons whose processes are perpendicular to the cortical surface. The analysis of the actual waveform of the EEG is very complicated because some of the postsynaptic potentials which cause it are excitatory

whereas others are inhibitory; some are near the surface of the cortex close to the recording electrode, others are deeper. Changes in EEG patterns are correlated with changes in behavior spanning the entire normal range from alertness to sleep. In general, there is a relationship between the degree of cerebral activating and the average frequency of the EEG rhythm, the frequency increasing progressively with higher and higher degrees of activity.

The intensities of the EEG waves on the surface of the brain may be as large as 10  $mV$ , whereas those recorded from the scalp have a smaller amplitude of approximately  $100\mu V$ . The frequencies of these brain waves range from 0.5 to 100 Hz and their character is highly dependent on the degree of activity of the cerebral cortex as mentioned above. For example, the waves change markedly between states of wakefulness and sleep. Much of the time, the brain waves are irregular and no general pattern can be observed. Yet at other times, distinct patterns do occur. Some of these are characteristic of specific abnormalities of the brain, such as epilepsy. Others occur in normal persons and may be classified as one of four wave groups: alpha, beta, theta, and delta, (see Fig-2) [8].

Alpha waves are rhythmic waves occurring at a frequency between 8 and 13 Hz. They are found in EEGs of almost all normal persons when they are awake in a quiet, resting state of cerebration. These waves occur most

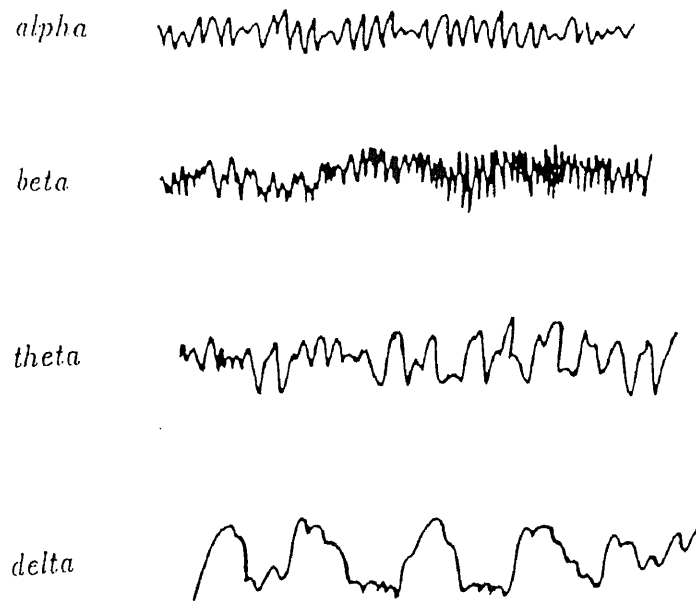


*Fig-2. Different types of normal EEG waves.*

intensely in the occipital region, but can also be recorded at times from the parietal and frontal regions of scalp. Their voltage is approximately  $20 \sim 200\mu V$ . When the subject is asleep, the alpha waves disappear completely. When the awake subject's attention is directed to some specific type of mental activity, the alpha waves are replaced by asynchronous waves of higher frequency, but lower amplitude, called beta waves.

*Beta waves* normally occur in the frequency range of 14 to 30 Hz, and sometimes -particularly during intense mental activity -as high as 50 Hz. These are most frequently recorded from the parietal and frontal regions of scalp. They can be divided into two major types: *Beta I* and *Beta II*. The

Beta I waves have a frequency about twice that of the alpha waves, and are affected by mental activity in much the same way as the alpha waves. The Beta II waves, on the other hand, appear during intense activation of the central nervous system or during tension. Thus one type of beta activity is elicited by mental activity, while the other is inhibited by it.

Theta waves have frequencies between 4 and 7 Hz. These occur mainly in the parietal and temporal regions in the children, but they also occur during emotional stress in some adults, particularly during the periods of disappointment and frustration. For example, they can often be brought about in the EEG of a frustrated person by allowing the person to enjoy some pleasant experience and then suddenly removing the element of pleasure. This causes theta waves for a while.

Delta waves include all the waves in the EEG below 3.5 Hz. Sometimes these waves occur only once every 2 or 3 s. They occur in deep sleep, in infancy, and in serious organic brain disease.

### **2.0.3 Clinical Measurement of the EEG**

When we make records of electrical potential difference between an exploring electrode resting on the cortical surface and a distant reference electrode, we are in effect recording the resultant field potential at a boundary of a large

conductile medium containing an array of active elements. It is evident from what is now known that under normal circumstances, conducted action potentials in axons contribute little to surface cortical records, since they usually occur asynchronously in time in large numbers of axons, which run in many directions relative to the surface. Thus their net influence on potential at the surface is negligible.

Electrophysiologists have shown that surface records show principally the net effect of local postsynaptic potentials of cortical cells. These may be either excitatory or inhibitory and may occur directly underneath the electrode or at some distance from it. A potential change recorded at the surface is a measure of the net potential drop between the surface site and the distant reference electrode. It is obvious, however, that if all the cell bodies and dendrites of cortical cells were randomly arranged in the cortical matrix, the net influence of synaptic current would be zero. Any electrical change recorded at the surface must be due to the orderly and symmetric arrangement of some class of cells within the cortex [9].

The system most often used to place electrodes for monitoring the clinical EEG is International Federation 10-20 system shown in Fig-3.

This system uses certain anatomical landmarks to standardize placement of EEG electrodes. Three types of electrode connections are commonly used:

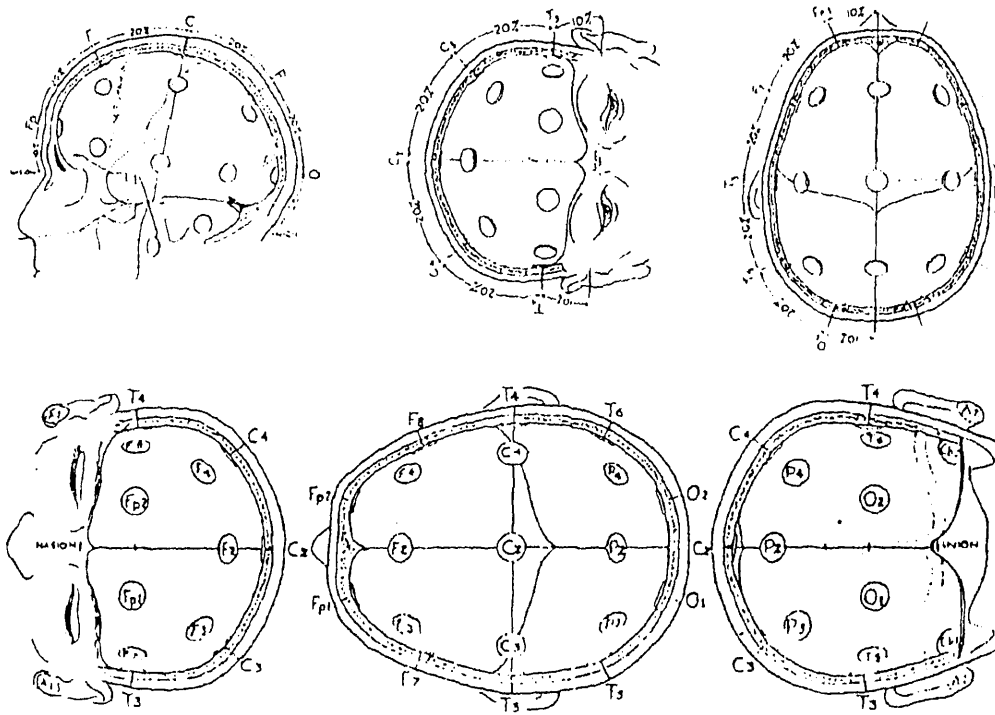


Fig-3 International 10-20 system.

Type A: between each of a pair (*bipolar*), Type B: between one monopolar lead and a distant reference electrode (*usually attached to both earlobes*), Type C: between one monopolar lead and the average of all, in which the system reference is formed by connecting all scalp-recording locations through equal high resistance to a common point. In the *bipolar* system, differential measurements are made between successive pairs of electrodes. The advantage of using a differential recording between successive pairs in the standard system is cancelation of far-field activity common to both electrodes, and thereby obtaining sharp localization of the response. In this project, we have chosen Type B.

In chapter 7, we will discuss measurement methods and experimental results.



# Chapter 3

## An A/D Converter

### 3.0.1 Introduction

Signals from an instrumentation tape recorder or directly from an EEG polygraph are analog signals. In order to perform digital processing by computers, there is a need for an interface between the analog signal and a computer. This interface in this project is the DASH-16.

The DASH-16 is a multifunction high speed analog/digital I/O expansion board for the IBM personal computers [10]. It is a full length board that is installed internally in an expansion slot of the IBM PC/XT/AT and turns the computer into a fast high precision data acquisition and analysis instrument.

Some of the features of the DASII-16 are listed below:

- 35,000 samples per second A/D with DMA.
- 16 single ended/8 differential analog input channels.
- Software included.
- Programmable scan rate.
- Bipolar and unipolar operation.

### 3.0.2 Hardware Configuration

By means of selectable function switches, the DASII-16 provides flexibility for the user. Before we program the DASII-16, it must be configured properly. In this project, the hardware configuration is set as follows:

FUNCTION	SWITCH	POSITION
INPUT CONFIGURATION	CHAN CFG	8
INPUT GAIN	GAIN	0.5
INPUT RANGE	BIP/UNI	BIP
DMA LEVEL	DMA	1
BASE ADDRESS	DIP	H300

We will describe these settings in detail in APPENDIX A.

### 3.0.3 Software Program

The DASH-16 can be programmed by using I/O input and output instructions. Most high level languages and assembly language have such equivalent instructions. However, in order to use such instructions, we have to fully understand the architecture of the DASH-16, deal with absolute I/O addresses and involve formatting data. Fortunately, a special I/O driver subroutine "DASH16.BIN" is provided to simplify some complicated program generation. This subroutine has such a format that the CALL routine in BASIC can access it. The various modes of the CALL routine can select all the functions of the DASH-16, including data format and error check. The CALL routine for "DASH16.BIN" is of the form :

```
CALL DASH16(MD%,DIO%,FLAG%)
```

Where MD% is interpreted as mode, DIO% as data and FLAG% as error.

Based on using "DASH16.BIN", the CALL routine can be used in 17 different modes. In this project, data acquisition requires four different modes:

**Mode 0:** Calling mode 0 is done in the initialization section of the program. The initialization provides the I/O location (that is the base address), interrupt and DMA levels before accessing any other mode. On entry the following parameters are assigned:

```
***10 DIO%(0) = &H300 (base address)
```

```
***20 DIO%(1) = 2 (interrupt level)
***30 DIO%(2) = 3 (DMA level)
***40 DASH16 = 0 (memory offset)
***50 MD% = 0 (mode 0)
***60 CALL DASH16(MD%,DIO%(0),FLAG%)
```

Here the base address is chosen as &H300 to match the D.I.P switch. Although we didn't use mode 5 and mode 6 which enable interrupts and the DMA controller, we still assign the usual value to interrupt variable DIO%(1) and DMA variable DIO%(2) for safety.

**Mode 1:** Mode 1 is used to set the scan limits of the multiplexer. This is done before performing an A/D conversion. In this project, we set default scan limits to be from channel 0 to channel 3 since we are converting four channel data. The scan limits can also be set interactively by the user.

**Mode 17:** Mode 17 is used to set the division ratios of Counter 2 and Counter 1 of the 8253 counter timer on the DASH16 board to produce the sampling rate. The counter input clock frequency is 1MHz from an on-board crystal oscillator. In this project, the default sampling rate is set to be 200Hz. The sampling rate can also be set interactively by the user.

**Mode 4:** Mode 4 can perform N A/D conversions and transfer data directly into a BASIC integer array. In this project, the default value is set

to be 1024 A/D conversions for each channel. The user may adjust the value of N interactively.

After A/D conversion, a data file is produced, which includes four-channel data. Furthermore, it is reformatted and plotted on the computer screen. This is shown in figure 4, which is an example of 4-channel EEG waves, recorded from a normal person, right-handed, age 25. These 2-second EEG waves are selected from the 5-minute EEG recordings in the eye-closed state.

The data are now ready for digital signal processing.

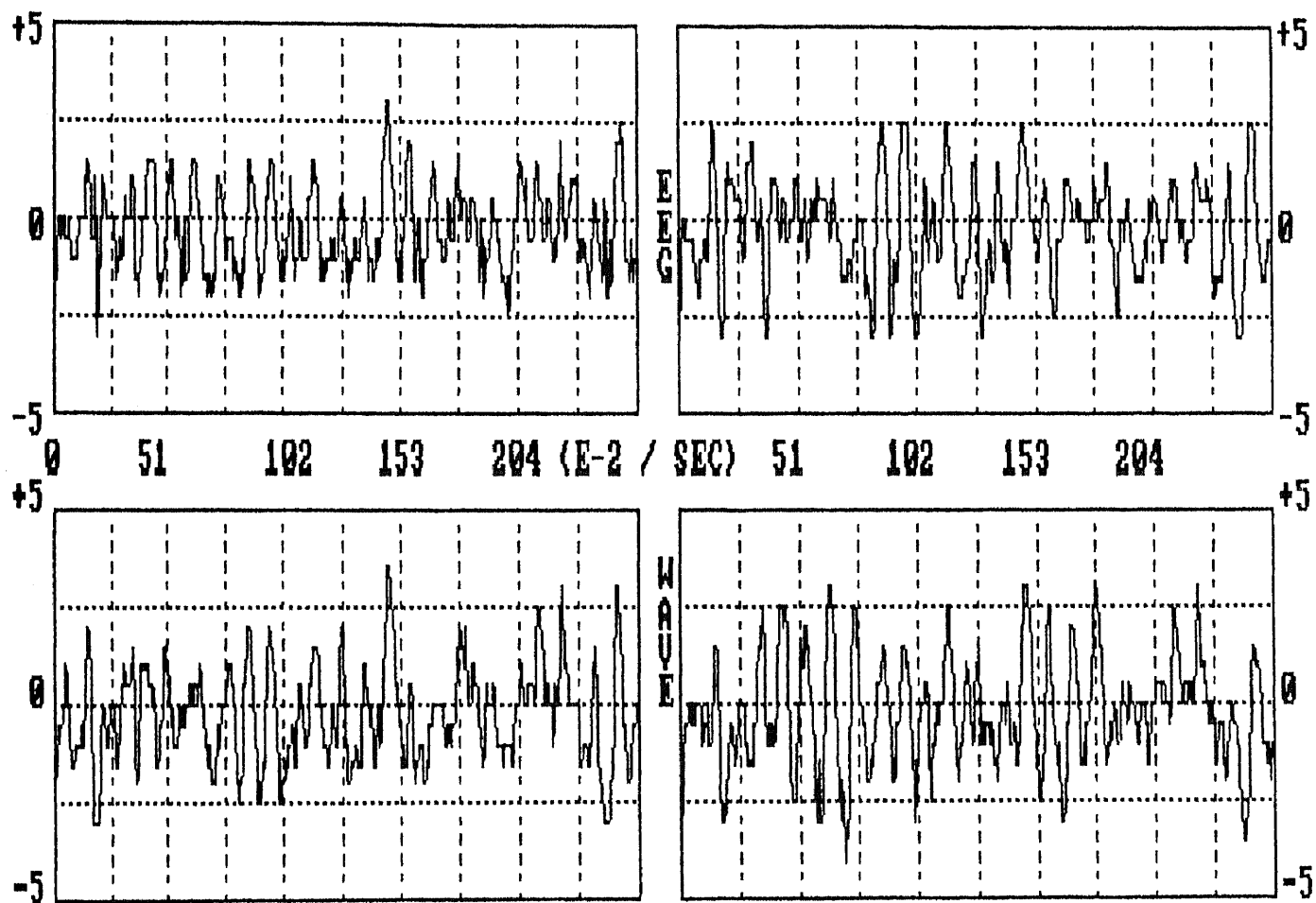


*Fig-4 four-channel normal EEG waves*

# Chapter 4

## Digital Signal Processing

### 4.0.1 Introduction

In chapter 2, we reviewed the features of the EEG. It is difficult to monitor the EEG signals in the time domain, especially in long recordings. However, the frequency of the EEG is often located in some range between 0.5 and 30 Hz, which mainly depends on the states of the brain and is defined as alpha, beta, theta and delta. Thus it is easy to grasp the useful information in the frequency domain instead of in the time domain. To find the frequency distribution of the EEG, we have to transform the time domain signal into the frequency domain. Therefore a Fourier transform is necessary. In this

chapter, we will discuss the Discrete Fourier Transform (DFT) and develop an efficient DFT algorithm, which is referred to as the Fast Fourier Transform (FFT).

## 4.0.2 The direct DFT computation

Basically, the DFT is a Fourier representation of a finite-length sequence which is itself a sequence rather than a continuous function, and corresponds to samples equally spaced in frequency of the Fourier transform of the signal. There are a number of points of view that can be taken toward the derivation and interpretation of the DFT representation of a finite-duration sequence [11][12]. Here we just give the results directly without any derivation.

The computational problem for the DFT is to compute the sequence  $X(k)$  of  $N$  complex-valued numbers given another sequence of data  $x(n)$  of length  $N$ , according to the formula:

$$X(K) = \sum_{n=0}^{N-1} x(n)e^{-j2\pi nK/N} \quad 0 \leq K \leq N-1 \quad (4.1)$$

In general, the data sequence  $x(n)$  is also assumed to be complex valued.

To simplify the notation, it is desirable to define the complex-valued phase factor  $W_N$ , which is an  $N$ th root of unity, as

$$W_N = e^{-j2\pi/N} \quad (4.2)$$



Then (4.1) becomes

$$X(K) = \sum_{n=0}^{N-1} x(n)W_N^{Kn} \quad 0 \leq K \leq N-1 \quad (4.3)$$

We observe that for each value of  $K$ , direct computation of  $X(K)$  involves  $N$  complex multiplications and  $N-1$  complex additions. Consequently, to compute all  $N$  values of the DFT requires  $N^2$  complex multiplications and  $N^2 - N$  complex additions.

It is generally accepted that a meaningful measure of complexity, or, of the time required to implement a computing algorithm, is the number of multiplications and additions required. Thus, for direct computation of the DFT, a convenient measure of the efficiency of the computation is the fact that  $4N^2$  real multiplication and  $4N(N-1)$  real additions are required. Since the amount of computation, and thus the computation time, is approximately proportional to  $N^2$ , it is evident that the number of arithmetic operations required to compute the DFT by the direct method becomes very large for large values of  $N$ . For this reason, computational procedures that reduce the number of multiplications and additions is of considerable interest.

In view of the computational problem of the DFT, the direct computation of the DFT is basically inefficient primarily because it doesn't exploit the symmetry and periodicity properties of the phase factor  $W_N$ . In particular,

these two properties are:

$$W_N^{k(N-n)} = (W_N^{kn})^* \quad (4.4)$$

$$W_N^{kn} = W_N^{k(n+N)} = W_N^{n(k+N)} \quad (4.5)$$

The computationally efficient algorithms described in the next section, known collectively as Fast Fourier Transform algorithms, exploit these two basic properties of the phase factor.

### 4.0.3 Fast Fourier Transform

The development of computationally efficient algorithms for the DFT is made possible if we adopt a divide-and-conquer approach [12]. The fundamental principle is based on the decomposition of the computation of the DFT of a sequence of length  $N$  into successively smaller discrete Fourier transforms. The manner in which this principle is implemented leads to a variety of different algorithms, all with comparable improvements in computational speed. Two basic classes of FFT algorithms are mostly of interest. The first is called decimation-in-time. In the process of arranging the computation into smaller transforms, the sequence  $x(n)$  is decomposed into successively smaller subsequences. The second is decimation-in-frequency. The sequence of discrete Fourier transform coefficients  $X(K)$  is decomposed into smaller subsequences. In this project, we have chosen the second class of FFT algorithm.

To derive this algorithm, we begin by splitting the DFT formula into two summations, one of which involves the sum over the first  $N/2$  data points and the second sum involves the last  $N/2$  data points. Thus we obtain:

$$X(K) = \sum_{n=0}^{(N/2)-1} x(n)W_N^{Kn} + \sum_{n=N/2}^{N-1} x(n)W_N^{Kn} = \sum_{n=0}^{(N/2)-1} x(n)W_N^{Kn} + W_N^{NK/2} \sum_{n=0}^{(N/2)-1} x(n+N/2)W_N^K \quad (4.6)$$

Since  $W_N^{KN/2} = (-1)^K$ , the expression (4.6) can be rewritten as

$$X(K) = \sum_{n=0}^{(N/2)-1} [x(n) + (-1)^K x(n+N/2)]W_N^{Kn} \quad (4.7)$$

Now, decimate  $X(K)$  into the even and odd numbered samples. Thus we obtain

$$X(2K) = \sum_{n=0}^{(N/2)-1} [x(n) + x(n+N/2)]W_{N/2}^{Kn} \quad (K = 0, 1, \dots, N/2 - 1) \quad (4.8)$$

$$X(2K+1) = \sum_{n=0}^{(N/2)-1} \{[x(n) - x(n+N/2)]W_N^n\} W_{N/2}^{Kn} \quad (K = 0, 1, \dots, N/2 - 1) \quad (4.9)$$

where we have used the fact that  $W_N^2 = W_{N/2}$ .

If we define the  $N/2$ -point sequences  $g(n)$  and  $h(n)$  as

$$g(n) = x(n) + x(n+N/2) \quad n = 0, 1, 2, \dots, N/2 \quad (4.10)$$

$$h(n) = [x(n) - x(n+N/2)]W_N^n \quad n = 0, 1, 2, \dots, N/2 - 1 \quad (4.11)$$

then

$$X(2K) = \sum_{n=0}^{(N/2)-1} g(n)W_{N/2}^{Kn} \quad (4.12)$$

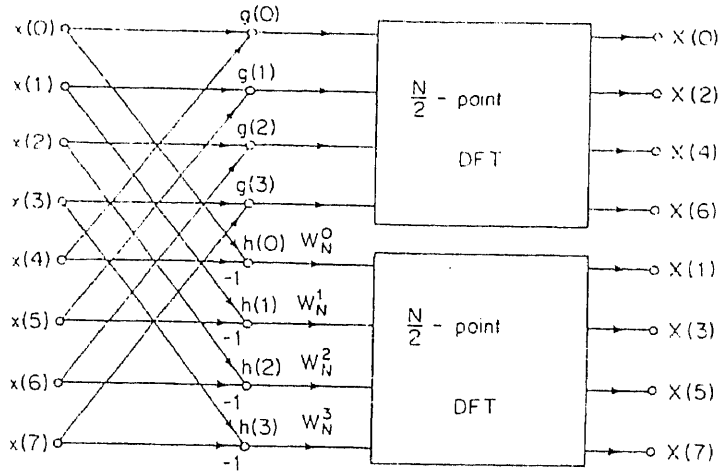


Fig-5 Computing the FFT

$$X(2K + 1) = \sum_{n=0}^{(N/2)-1} h(n)W_{N/2}^{Kn} \quad (4.13)$$

The computation of the sequence  $g(n)$  and  $h(n)$  according to (4.10) and (4.11) and subsequent use of these sequences to compute the  $N/2$ -point DFTs are depicted in Fig-5. We observe that the basic computation in this figure involves the butterfly operation illustrated in Fig-6.

The computational procedure above can be repeated through decimation of the  $N/2$ -point DFTs  $X(2K)$  and  $X(2K+1)$ . The entire process involves  $L = \log_2 N$  stages of decimation, where each stage involves  $N/2$  butterflies of the type shown in Fig-6. Consequently, the computation of the  $N$ -point DFT via the decimation-in-frequency FFT algorithm requires  $(N/2)\log_2 N$  complex

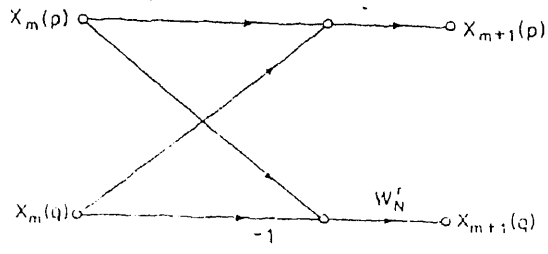


Fig-6 Butterfly operation

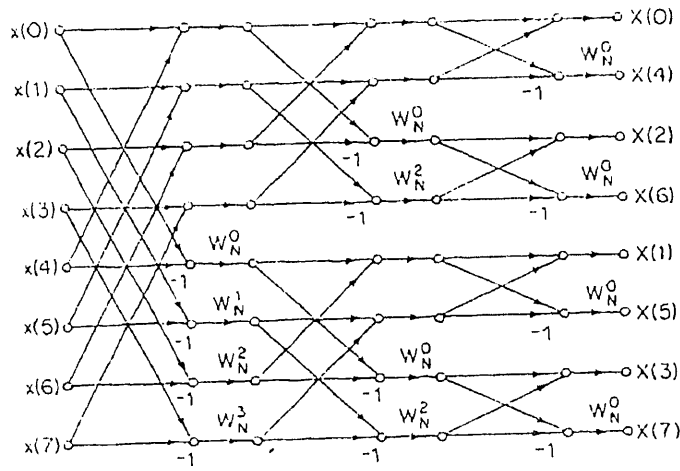


Fig-7 Eight-point FFT computation

multiplications and  $N \log_2 N$  complex additions. For illustrative purposes, the eight-point decimation-in-frequency algorithm is given in Fig-7.

With the help of this signal processing algorithm, a radix-2 FFT program has been developed, which can transform the 4-channel sampled data in the time domain into the frequency domain. A subroutine has also been used to obtain the power spectra of the 4-channel FFT.

Because the N-point FFTs of four sequences in this project are to be computed, it is inefficient to recompute the phase factors each time. It is more efficient to compute the phase factors once and to store them in “a table” in memory. This is called a table-look-up technique, which is the best way to deal with the phase factors in such four-channel FFT processing.

We observe from Fig-7 that the input data  $x(n)$  occurs in natural order, but the output FFT occurs in bit-reversed order. Thus it is necessary to use a bit-reversal subroutine to restore the FFT natural order.

Figure 8 shows the power spectra of the ECG wave shown in fig-4. The magnitudes of the 4-channel spectra have been normalized, and vertical values in fig-8 correspond to the different colors. The maximum value is 15 since we use 15 different colors. The horizontal axes shows the frequency scale, whose maximum value is 100 Hz since we chose 200 Hz as the sampling rate.

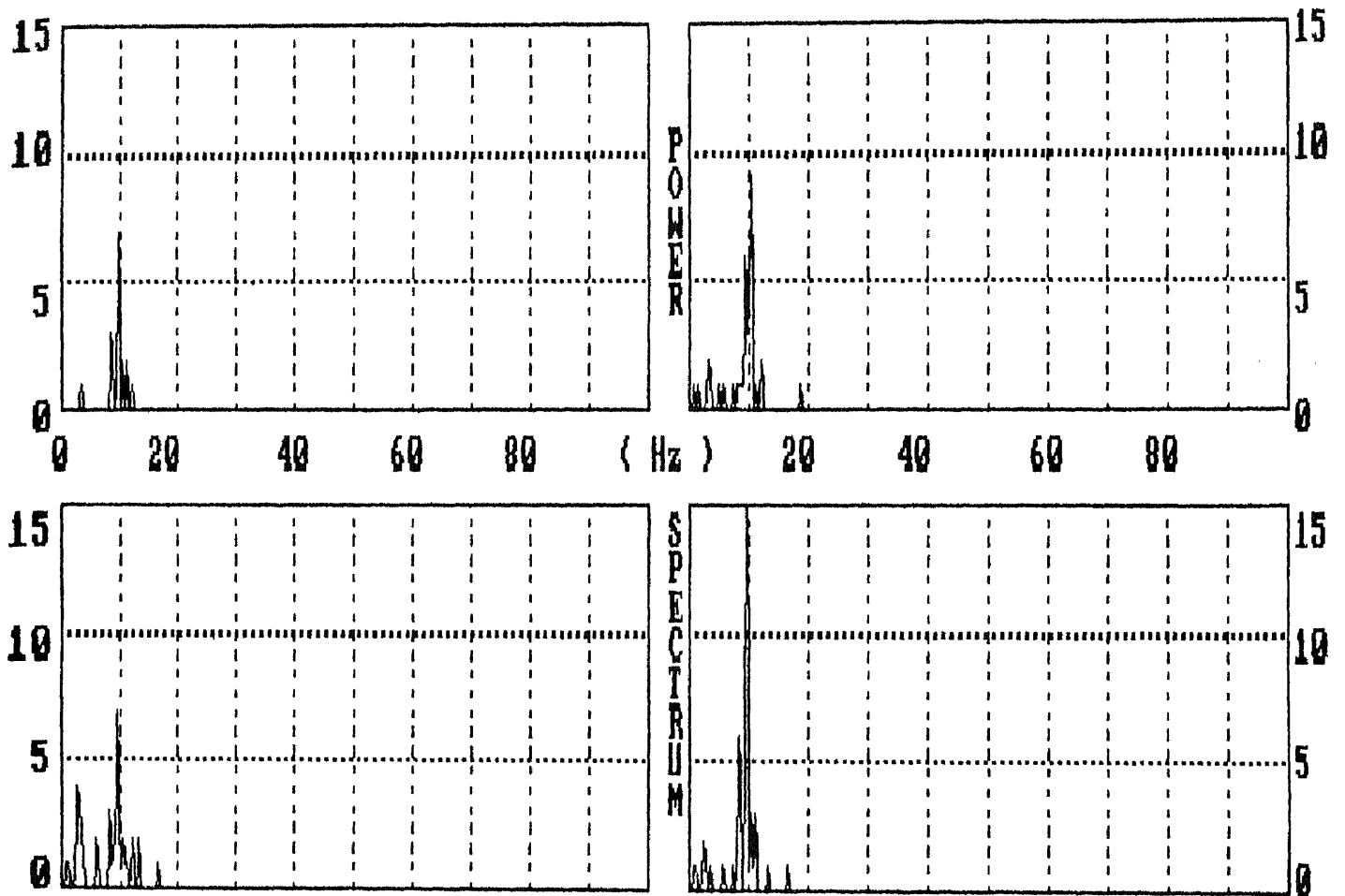


*Fig-8 4-channel power spectra of normal EEG*

# Chapter 5

## CRT Controller in The PC

### 5.0.1 Introduction

In chapter 4, we have discussed how to obtain the EEG power spectrum. However analysis of these EEG power spectra is still difficult because they present too much information to be easily grasped by visual inspection alone. A method was described by Frank H. Duffy in 1979 [4], in which EEG spectral energy in any EEG band, i.e., alpha, beta, theta and delta, was displayed within a graphic outline of the head by means of topographic mapping. This technique is usually called BEAM.

Numerous attempts have been made to create such a mapping environ-



ment with the recent development of computers [2][3][14]. A new interest in personal computerized topographic mapping seems to be developing. The reason may be that the PC has many powerful graphics functions, and is inexpensive. In addition, the recent introduction of advanced microprocessors such as the 286, 386 and math-coprocessors such as the 287, 387 in personal computers greatly increases the PC's computational speed. Thus in this project, we have used the PC not only to process data, but also to produce a topographic mapping environment.

In this project, we have created a mapping environment with  $100 \times 80$  resolution in 16 different colors on both the Fountain PC/XT with a Color Graphics Adapter (CGA) and an AT&T PC/AT with an Enhanced Graphics Adapter (EGA), or their compatible computers.

Generally most high-level languages work in text or graphics modes. In text mode, there are usually two kinds of resolution, one is  $80 \times 25$  in 16 colors, called the high-resolution mode; the other is  $40 \times 25$  in 16 colors, called the low-resolution mode. In graphics modes, there are usually two kinds of resolution, one is  $320 \times 200$  in 4 colors at a time, called medium-resolution; the other is  $640 \times 200$  in black and white, called the high-resolution mode [13]. For text modes, the resolution is too low to be useful for our purpose. For graphics modes, the resolution is enough, but the color set is not enough

to code the EEG data for mapping purposes. It is obvious that the more colors we can use, the more precisely the EEG data can be coded. Therefore, it is necessary to create a new mode with acceptable resolution in as many colors as needed.

To create a new mode, we have to deal with the graphics adapters via I/O ports. In a PC/XT (or compatible), the screen resolution and attributes are usually controlled by the Color Graphics Adapter. In the PC/AT (or compatible), the screen resolution and attributes are controlled by the Enhanced Graphics Adapter. In this chapter, we will discuss how to program both CGA and EGA boards and how to exploit their CRT controllers to produce a new mode with  $100 \times 80$  resolution in 16 different colors. The principle of this technique is changing the horizontal timing and vertical timing parameters, and forcing a text mode (high-resolution mode) into a new “text mode” with 100 lines  $\times$  80 columns. That is, the number of vertical lines in the high resolution text mode is increased 4 times. Since the I/O ports and their registers for CGA and EGA are quite different, we will discuss them in different sections.

## 5.0.2 CGA

The Color Graphics Adapter is one of the original display adapters in the IBM PC family. It is designed to show both text characters and pictures (graphics) drawn from a series of fine dots [13]. Although CGA is able to show as many as 16 colors and has several display modes that provide a variety of combinations of colors and screen resolutions, it doesn't have an available mode for our special purpose as discussed previously.

The special programming in this project uses the OUT command in BASIC to send bytes to a special set of addresses housed in the I/O space of the computer. Using this BASIC command enables us to access the I/O space directly, and thus program the CGA and its video controller.

As we indicated above, we are communicating directly with the adapter board and its video controller through I/O ports. There are many I/O ports in a computer. These I/O ports are individual addressable 8-bit cells and help the programmer interface with such devices as printers, keyboards, communication lines and video boards. Through the IBM PC Technical Reference Manual, we find seven I/O ports that are used to access the CGA. Only four of them are useful to us. They are shown in table 1.

Table 1

Address in Hex	Description
3D0	6845 Index Register
3D1	6845 Data Register
3D8	Mode Control
3D9	Color Control

Of the four useable ports, 3D0/3D1 provide direct access to the Motorola 6845 video chip, and 3D8/3D9 are used to set certain bits on other parts of the adapter board.

It is worth giving a brief description of the Motorola 6845 video chip here because our major effort is to program this chip on the CGA. The Motorola 6845 video chip lies at the heart of the CGA. Its main function is to provide the horizontal and vertical synchronization video signals and the digital address that scans through the video RAM as a picture is being displayed. This video chip also provides information for scanning through the rows of the dot matrix for each row of characters.

The Motorola 6845 has 18 internal 8-bit registers. These registers can be individually programmed by loading values into them. These registers hold such information as the number of bytes per line and the number of lines that are displayed on the screen. Normally, the computer automatically loads these registers upon start-up and whenever we change the modes.

In table 1, we show the two port addresses 3D0/3D1, which are used to

do our special programming of the 6845 video chip. Through the two ports, we send bits to some of 18 internal registers of the 6845 video chip to change timing parameters.

**PORT 3D0** is the index register. Its function is to set up a communication channel or pathway. The number sent to this port selects which of the 18 internal registers to access next. These 18 internal register are shown in table 2. Of these 18 internal registers, we are interested only in ten of them, that is, from Register 0 to Register 9.

Table 2

Register No	Function	Value
0	Horizontal Time Total	113
1	Horizontal Bytes Displayed	80
2	Horizontal Synchronization Position	90
3	Horizontal Synchronization Width	10
4	Vertical Lines Total	127
5	Vertical Adjust	6
6	Vertical Lines Displayed	100
7	Vertical Synchronization Position	106
8	Interlace Mode	0
9	Maximum Scan Line	1
10	Cursor Start	*
11	Cursor End	*
12	Memory Start Address (high)	*
13	Memory Start Address (low)	*
14	Cursor Address (high)	*
15	Cursor Address (low)	*
16	Light Pen (high)	*
17	Light Pen (low)	*

**PORT 3D1** is the data register. After 3D0 selected a register, the value

to be changed will be sent to this port (see APPENDIX B for detail).

PORT 3D8 has six important bits which control the status of the CGA board. Their functions and values used in this project are listed in table 3.

Table 3

Bit	0	1	value
0	40 columns	80 columns	1
1	Text	Graphics	0
2	Color	Black and White	0
3	No picture	Normal Picture	1
4	mediaum resolution	high resolution	0
5	Blinking	Intensity	0

PORT 3D9 contains bits that set background and border colors. We set this port for a green border.

We can use the OUT command in BASIC to send the information we want to the corresponding port to produce a new mode. In this technique, our major effort is to make the text mode to be suitable for graphics purposes. Other techniques may be found to reach the same goal, and these will be discussed later.

Since we have a new mode, we need to develop a new plotting subroutine. This subroutine will calculate the addresses of the character attributes and pick up the corresponding colors from them.

In text mode, a character needs two bytes, one is for ASCII code, the other for attribute. For any given character position, we can use the following

formulas to compute the position of the corresponding bytes in video RAM:

$$ASCII : (80 \times row + column) \times 2$$

$$Attribute : (80 \times row + column) \times 2 + 1$$

Hence the subroutine for this new mode is:

$$M = 160 * Y + 2 * X + 1$$

POKE M,16 \* C

where X,Y are coordinates for line and column, C is color value.

This new mode is only used on the Fountain PC/XT with a CGA or compatible computers. With the recent needs of high-resolution graphics and high-computational speed in science and engineering research, more advanced computers (called AT computers) with 286 and 386 microprocessors have mostly adopted the Enhanced Graphics Adapter as video boards. Some advanced computers even have Video Graphics Array (VGA) inside, which is a new, more advanced and complex graphics standard. We will discuss the EGA in the next section.

### 5.0.3 EGA

Since its introduction in late 1984, the Enhanced Graphics Adapter has become the graphics standard in the IBM personal computer world. The EGA is IBM's effort to unify the variety of display adapters and extend the PC

family's capabilities into new technology. The EGA essentially combines all the features of the Monochrome Adapter (MD), the Color Graphics Adapter (CGA) and the Hercules Card, with some new modes that can be used with high-quality color monitors. It is clear that EGA is a single display adapter which combines all the advantage of other boards. For example, EGA covers all the CGA modes with its own unique modes. Since it has more modes, which need more registers on the video board, programming EGA becomes more complicated.

On the EGA, the Cathode Ray Tube Controller (CRTC) plays a major role in controlling the resolution and attributes of the computer screen. Although most of the CRTC registers replicate the functions of the 6845 controller found on the CGA, there are still a few differences. In addition, the I/O addresses of these two adapters are different, and the two 3D8 and 3D9 two ports used by the CGA are not used by the EGA. Because of these differences, the mode-setting program for the CGA doesn't work on the EGA board. Hence, a new mode-setting program for EGA is needed if we want to use a computer with an EGA board.

The CRTC has two I/O ports, 3D4/3D5 (16). Through these two ports, we can control the horizontal and vertical timing parameters to produce a new mode for our purpose with  $100 \times 80$  resolution in 16 different colors.



PORT 3D4 is a CRTC index register. It selects which register will appear at port 3D5. It sets up a path channel for changing the timing parameters. The index and function of port 3D4 are listed in table 4.

Table 4

Index of Register	Function	Value
0	Horizontal Total	112
1	Horizontal Display End	79
2	Start Horizontal Blanking	92
3	End Horizontal Blanking	47
4	Start Horizontal Retrace	95
5	End Horizontal Retrace	7
6	Vertical Total	4
7	Overflow	3
8	Preset Row Scan	0
9	Max Scan Line	2
10	Cursor Start	*
11	Cursor end	*
12	Start Address (high)	*
13	Start Address (low)	*
14	Cursor Location (high)	*
15	Cursor Location (low)	*
16	Vertical Retrace Start (write)	47
16	Light Pen High (read only)	*
17	Vertical Retrace End (write)	99
17	Light Pen Low (read only)	*
18	Vertical Display End	205
19	Offset	*
20	Underline Location	*
21	Start Vertical Blanking	*
22	End Vertical Blanking	*
23	Mode Control	*
24	Line Compare	*

Of these 24 registers we are interested in thirteen of them, that is, from

Index 0 to Index 9 and from Index 16 to Index 18.

**PORT 3D5** is a data register. When port 3D4 selects a register by loading the index number, the value to be changed is written to port 3D5. (see APPENDIX C for detail).

When we set all the registers properly by means of the OUT command in BASIC, a nice mapping environment was produced, consisting of  $100 \times 80$  resolution in 16 different colors. The following plotting subroutine was used:

```
M = 160 * Y + 2 * X : POKE M,219
```

```
M = M + 1 : POKE M,C
```

where X,Y are the coordinates of a pixel and C is the color number.

#### 5.0.4 Discussion

In this chapter, we have discussed how to exploit a new mode by programming the CGA/EGA. This technique is not limited to the BASIC language. We can use any high-level language with I/O commands as well as assembly languages. The reason we chose BASIC is that we want this program to be compatible with the data acquisition and the digital signal processing programs. Thus it is automatic from data acquisition to final mapping.

It initially seemed impossible to pick up 16 different colors at a time in the graphics modes on the CGA. However, if we are familiar with how a character

is mapped on the screen [13], we can find many ways to set a new mode for graphics with 16 colors. Our project is an example. Another possible way is to convert the normal medium resolution graphics mode ( $320 \times 200$ ) with 4 colors into a low-resolution mode ( $160 \times 200$ ) with 16 colors. This will sacrifice the resolution for more colors. The basic technique is to use one color clock to plot two horizontal pixels which comprise one pixel in the new mode. The subroutine in BASIC is as follows:

```
### 10 C1 = C/4
### 20 C2 = C MOD 4
### 30 PSET (2 * X,Y),C1
### 40 PSET (2 * X+1,Y),C2
### 50 RETURN
```

where  $X,Y$  are the coordinates of a pixel in the new mode and  $C$  is the color number which may be one of four colors in the medium-resolution mode.  $C1$  is the low 2 bits of a color and  $C2$  is the high 2 bits of a color. During a color clock, The  $(2X,Y)$  position is plotted by the low 2 bits of a color while the  $(2X+1,Y)$  position is plotted by the high 2 bits of a color. Thus, the new position formed by  $(2X,Y)$  and  $(2X+1,Y)$  in the new mode will have 16 possibilities of different color choices. It is obvious that this technique is simpler than what we discussed previously. However, the size

of our topographic map needs a screen with about  $60 \times 60$  resolution, and the resolution in this mode is so high that the size of a picture will become very small. If we want to keep the same mapping size in this mode, the computational time for each picture will increase greatly.

It seems easy to pick up 16 colors at a time in the graphics mode on the EGA since there are two modes (mode 13 and mode 14) which are of  $320 \times 200$  resolution in 16 colors and of  $640 \times 200$  resolution in 16 colors. Since our topographic map needs only  $60 \times 60$  resolution, these two modes are not suitable for our purpose. If we are working in such a mapping environment with a  $60 \times 60$  matrix, the head map is too small to be clear. If we are using a larger mapping frame, for instance,  $180 \times 180$ , the computing time will increase  $(180 \times 180)/(60 \times 60) = 9$  times as much as what we discussed before. Thus it is reasonable to exploit the new mode instead of using default modes.

Therefore, for a good environment, three factors must be considered: (1) colors to be used, which should be enough for precise mapping; (2) resolution, which should be reasonable, acceptable and not time-consuming; (3) topographic map, which should be continuous and as smooth as possible with the consideration of the time-cost and speed. We will discuss details of the third item in chapter 6.

# Chapter 6

## Topographic Mapping

### Techniques

#### 6.0.1 Introduction

The goal of enhancing the visibility of EEG data has led to the use of scalp surface distribution mapping. These maps transform apparently complex power spectra wave forms into rather simple surface distributions (i.e. pictures) and allow readily extraction of useful clinical information. However, EEG data are recorded at only a few isolated electrode sites. To present the overall surface distribution on the entire scalp it is necessary to interpolate

between the electrodes. This chapter will introduce three popular mathematical tools for the interpolation, i.e., linear interpolation [4], four nearest neighbors (4-N-N) [14] and surface spline methods [15] which we have adopted in this project.

### 6.0.2 A Linear Interpolation Method

From an interpolation point of view, it may be desirable to interpolate values in a plane determined by the three known points. This method is called linear three-dimensional interpolation. Mathematically, the requirement for setting up the solution of the interpolation formulas is determination of the equation of this plane to which the interpolated points will be projected. It is the simplest mathematical tool for interpolation.

Let  $n$  be the number of electrodes,  $e_i = (x_i, y_i)$  the coordinates of the  $i$ th electrode on the scalp surface, and  $z_i$  the value of the spectral energy at the electrode  $e_i$ . Assume an arbitrary point to be  $e = (x, y)$  in the scalp surface, and the linearly interpolated value at  $e = (x, y)$  to be  $z$ . The general form of the equation of a plane is :

$$Ax + By + Cz = D \tag{6.1}$$

We will substitute k coefficients for A, B, C, and D as follows :

$$k_{10}x + k_9y + \frac{k_8}{k_7}z = 1 \quad (6.2)$$

The following definitions are then used (18):

$$k_1 = x_2y_1 - x_1y_2 \quad (6.3)$$

$$k_2 = x_2z_1 - x_1z_2 \quad (6.4)$$

$$k_3 = x_2 - x_1 \quad (6.5)$$

$$k_4 = x_3y_1 - x_1y_3 \quad (6.6)$$

$$k_5 = x_3z_1 - x_1z_3 \quad (6.7)$$

$$k_6 = x_3 - x_1 \quad (6.8)$$

$$k_7 = k_4k_2 - k_1k_5 \quad (6.9)$$

$$k_8 = k_4k_3 - k_1k_6 \quad (6.10)$$

$$k_9 = \frac{k_3 - \frac{k_2k_8}{k_7}}{k_1} \quad (6.11)$$

$$k_{10} = \frac{1 - k_9y_1 - \frac{k_8}{k_7}z_1}{x_1} \quad (6.12)$$

Finally,

$$z = \frac{k_7}{k_8}(1 - k_{10}x - k_9y) \quad (6.13)$$

where  $e_1 = (x_1, y_1)$ ,  $e_2 = (x_2, y_2)$ ,  $e_3 = (x_3, y_3)$  are the three nearest electrodes to  $e = (x, y)$ , and  $z_1, z_2, z_3$  are their values of the spectral energy.

In mathematics, there may be a default condition such as would occur if  $x_1, k_1$ , or  $k_7$  were zero. In practice, if we define the position of electrodes properly, we can avoid this condition.

### 6.0.3 4-Nearest Neighbors Method

4-Nearest Neighbors method (4-N-N) is a classical interpolation method. It is a simple and nonlinear method.

Let  $e = (x, y)$  denote the coordinate of an arbitrary point on the scalp,  $e_i = (x_i, y_i)$ , with  $i = 1, 2, 3, 4$ , its 4 nearest electrodes and  $d_i$  ( $d_i^2 = (x - x_i)^2 + (y - y_i)^2$ ) the distance between  $e$  and  $e_i$ . The 4-nearest neighbors interpolation formula is given by equation (6.14) [15]:

$$z = \frac{\sum_{i=1}^4 z_i d_i^m}{\sum_{i=1}^4 d_i^m} \quad (6.14)$$

where  $z$  is the value at  $e = (x, y)$  and  $z_i$  is the value at  $e_i = (x_i, y_i)$ ,  $m$  represents the  $m$ th degree of 4-N-N interpolation.

From the formula, it follows that extrema are always located at the electrode positions.

### 6.0.4 Surface Spline Method

A surface spline is the surface obtained by minimizing the bending energy of an infinite plate constrained to pass through known points. This method



has been used for interpolating wing deflections in aerospace calculations. However, it was introduced to the mapping of scalp potentials by F. Perrin in 1987 [15].

Let  $e_i = (x_i, y_i)$  with  $i = 1, 2, 3, 4$ , be the coordinate of the  $i$ th electrode on the scalp, and  $z_i$  the value of the spectral energy at electrode  $e_i$ . For an arbitrary point  $e = (x, y)$ , its value is assumed to be  $z$ . Then, the  $m$ th degree surface spline interpolating formula is [15]:

$$z = \sum_{i=1}^4 p_i k_{m-1}(x - x_i, y - y_i) + q_{m-1}(x, y) \quad (6.15)$$

where

$$q_{m-1}(x, y) = \sum_{d=0}^{M-1} \sum_{k=0}^d q_{kd} x^{d-k} y^k \quad (6.16)$$

$$k_{m-1}(s, t) = (s^2 + t^2)^{m-1} \log(s^2 + t^2) \quad (6.17)$$

Let

$$Q = (q_{00}, q_{01}, \dots, q_{m-1, m-1})' \quad (6.18)$$

$$P = (p_1, p_2, p_3, p_4)' \quad (6.19)$$

$$Z = (z_1, z_2, z_3, z_4)' \quad (6.20)$$

then  $Q$  and  $P$  are the solution of the following matrix equations:

$$K \cdot P + E \cdot Q = Z \quad (6.21)$$

$$E' \cdot P = 0 \quad (6.22)$$

where

$$K = (k_{ij}) = k_{m-1}(x_i - x_j) \quad (6.23)$$

$$E = \begin{pmatrix} 1 & x_1 & y_1 & x_1^2 & x_1 y_1 & \dots & x_1 y_1^{m-2} & y_1^{m-1} \\ 1 & x_2 & y_2 & x_2^2 & x_2 y_2 & \dots & x_2 y_2^{m-2} & y_2^{m-1} \\ 1 & x_3 & y_3 & x_3^2 & x_3 y_3 & \dots & x_3 y_3^{m-2} & y_3^{m-1} \\ 1 & x_4 & y_4 & x_4^2 & x_4 y_4 & \dots & x_4 y_4^{m-2} & y_4^{m-1} \end{pmatrix} \quad (6.24)$$

In this project, we have chosen a 2nd degree surface spline and electrode sites are defined as (15,30), (30,15), (45,30) and (30,45). By solving the above equations, we have obtained the following resulting formulas:

$$H_1 = [(x - 15)^2 + (y - 30)^2] \log[(x - 15)^2 + (y - 30)^2] \quad (6.25)$$

$$H_2 = [(x - 30)^2 + (y - 15)^2] \log[(x - 30)^2 + (y - 15)^2] \quad (6.26)$$

$$H_3 = [(x - 45)^2 + (y - 30)^2] \log[(x - 45)^2 + (y - 30)^2] \quad (6.27)$$

$$H_4 = [(x - 30)^2 + (y - 45)^2] \log[(x - 30)^2 + (y - 45)^2] \quad (6.28)$$

$$H(x, y) = H_1 - H_2 + H_3 - H_4 \quad (6.29)$$

$$L = \frac{z_1 + z_2 + z_3 + z_4}{2495.33} \quad (6.30)$$

$$Q_0 = \frac{5z_1 + 5z_2 - 3z_3 - 3z_4}{4} \quad (6.31)$$

$$Q_1 = \frac{z_3 - z_1}{30} \quad (6.32)$$

$$Q_2 = \frac{z_4 - z_2}{30} \quad (6.33)$$

$$z = L \cdot H(x, y) + Q_0 + Q_1x + Q_2y \quad (6.34)$$

It is obvious that the more electrodes we use, the more complicated are the formulas we will have.

### 6.0.5 Discussion

In this paper, we have introduced three interpolation methods. We have experimented with all three methods. Among them, the linear interpolation method is simplest mathematically. It takes the least computational time and the color distribution in the head region is continuous. The disadvantage is that the topographic mapping is not very smooth. The 4-N-N method presents easy computation, less computational time than the surface spline interpolation method. However, the color map is discontinuous and extrema are always located at electrode sites. The mapping smoothness is not as good as surface spline interpolations. The surface spline method gives a continuous and the smoothest topographic mapping. In addition, with the increase of the degree, this method presents smoother mapping distribution. However, this advantage is at the expense of a lengthier computing time. On the other hand, to use the previous formulations (from (6.25) to (6.34)), the coordinates of the electrodes are restricted to be symmetrical.

In comparison to the linear and the 4-N-N interpolation methods, we

found the surface spline method is best for our purpose. The reason is that when we have specified the positions of electrodes on the head region properly, a table-look-up technique can be introduced to considerably reduce the computing time. Hence the mapping time doesn't increase much with regard to the fastest linear interpolation.

# Chapter 7

## Experiments and Results

### 7.0.1 General Description

The purpose of this project is to develop a method for EEG topographic mapping. In order to verify this method, several experiments were designed to display the following aspects:

- 1). to map the EEG in normal and pathological cases;
- 2). to compare the results of our experiments with the physician reports;
- 3). to investigate the usefulness of this method;
- 4). to offer suggestions for later exploration.

## 7.0.2 Subjects and Methods

This project is based on the background EEG power spectra mapping from 6 right-handed volunteers, one normal person, male, age 25; four male patients and one female patient, mean age 42.4.

In the routine of recording the EEGs, the surface of the scalp is prepared by first degreasing the recording areas by cleaning them with alcohol, then applying a conducting paste. A set of 7 gold disk electrodes are glued to the scalp, and held in place with a piece of cotton. Of these 7 electrodes, four input electrodes are placed on  $C_3$ ,  $C_4$ ,  $F_z$  and  $P_z$ , based on the international 10-20 system; two reference electrodes are placed on the ear lobes; one ground electrode is placed on the forehead. The potentials from the input electrodes are amplified by high-gain, differential, capacitively coupled amplifiers (BECKMAN R511A). The output signals are fed to a 4-channel Sony tape recorder. Filters between inputs and outputs are used to limit the frequency responses to the range of 0.5 to 30 Hz.

The EEGs are recorded with the subject awake, but resting and lying on a reclining chair with eyes closed. With the patient relaxed in such a manner, artifacts from electrode-lead movement and eye blinking are significantly reduced. Otherwise muscle activity from face, neck, ears, etc., is a contaminant of the EEG records.

The 4-channel EEGs recorded on the audio tape are digitized at 200 samples per second. A pre-processing program is used to remove the d.c. components in the sampled data, and plot the 4-channel wave forms on one screen. A digital signal processing program is then used to obtain the 4-channel EEG power spectra. Finally, the values in 2 Hz frequency bands between 5 and 21 Hz are selected, coded in different colors from white (low power) to dark blue (high power) and mapped on the color monitor by a mapping program. The areas around the electrodes are filled by the surface spline interpolation.

### **7.0.3 Results**

The configuration of the brain map in this project is shown in fig-9. BEAM spectral plots for six subjects in eyes-closed state are printed in color hard-copies (BEAM pictures, see fig-10 – fig-15), in which plots from 5 – 21 Hz are shown. In these figures, 5-7 Hz and 7-9 Hz are the theta bands; 9-11 and 11-13 Hz are the alpha bands; 13-15 Hz, 15-17 Hz, 17-19 Hz and 19-21 Hz are the beta bands. We propose that asymmetry, low activity (light colors) and high activity (deep colors) compared to the normal subject may represent some kind of brain dysfunction or disease. We will now describe our results and corresponding physician's reports without any discussion. In the

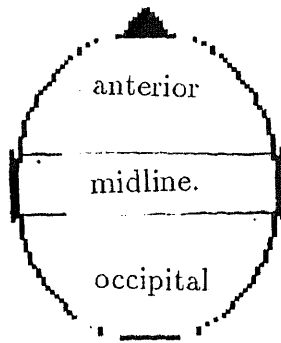


*fig-9 Configuration of the brain map*

following section, we will discuss the results and draw conclusions.

**Subject 1:** Figure 10 displays the BEAM pictures for a normal person without any abnormal neurological history. In the 7-9 Hz band, the electrical activity in the anterior region is lower than in the occipital region; in the 9-11 Hz band, the maximal activity is located in the occipital region, and the activity in anterior region appears high; in the 11-13 Hz band, the occipital region activity tends to be maximal, and low activity occurs in the midline region. It should be noted that the activity between left brain and right brain of the normal subject is in balance, i.e., the BEAM pictures are symmetrical.

**Subject 2:** Figure 11 illustrates the BEAM pictures for a patient with the history of cerebral ischemia, and coronary by-pass surgery. It is noted that asymmetry occurs in the 5-7 Hz band, slight asymmetry in the 9-11 Hz and the 11-13 Hz bands, symmetry in the 7-9 Hz and the 13-15 Hz bands. The slow activity is increased. The low activity in the 7-9 Hz band occurs in the midline region.

Based on the EEG reports, no asymmetry exists for this subject, and



the EEG waveforms are normal. According to the magnetic resonance imaging (MRI) reports, subject 2 has mild ventriculomegaly with minimal white matter disease.

**Subject 3:** Figure 12 shows the BEAM pictures for a patient with the problems of headaches with vascular sinusitis and a history of seizure. It is noted that slow activity is increased. The plot in the 5-7 Hz band demonstrates a slightly higher activity in the left brain. The anterior region activity in the bands between 5 and 11 Hz is high.

Based on the EEG reports, the EEG waveforms are normal, low voltage record, no asymmetry. According to the MRI reports, for subject 3, a small chronic hemorrhage in the left posterior parietal lobe is found.

**Subject 4:** Figure 13 displays the BEAM pictures for a patient with the history of headaches on the left side following a concussion. The plot in the 9-11 Hz band demonstrates a greatly decreased activity. A slightly asymmetry occurs in the 7-9 Hz band. The plot in the 5-7 Hz band is asymmetrical and shows a high activity in the anterior region and a color discontinuity in the left frontal brain.

Based on the EEG reports, the EEG waveforms are normal, and no indication of asymmetry is present. According to the MRI reports, subject 4 has the post traumatic encephalomalacia of the left frontal lobe.

**Subject 5:** Figure 14 illustrates the BEAM pictures for a patient with a history of cerebral concussion, contusion of the left orbit and neck area and post traumatic anxiety. The plot in the 9-11 Hz band demonstrates a slight asymmetry and a high activity in the left brain.

Based on the EEG reports, the EEG waveforms are normal, no asymmetry. Subject 5 has no MRI reports.

**Subject 6:** Figure 15 displays the BEAM pictures for a patient with problems of memory impairment and mild-moderate depression. A decreased fast activity is noted, with a slight asymmetry in the 9-11 Hz band. The power level at the electrode sites in the midline and anterior is the same.

Based on the EEG reports, the EEG waveforms show no asymmetry. According to the MRI reports, for subject 6, there is a right basal ganglia lacunar infarct and questionable left cerebral penduncle infarct.

#### **7.0.4 Discussion**

Interpretation of the multichannel EEG is both difficult and time-consuming because it needs electroencephalographers to correlate the amplitude and time-period over a large amount of EEG recording. With the computerized mapping of the multichannel EEGs, a large amount of EEG data is consolidated into a few pictures. These BEAM pictures can provide more

information than the EEG reports. Based on the EEG reports, four patients have no asymmetry between their left and right brains, one patient is uncertain. According to our experiments, the BEAM pictures for these five patients demonstrate at least some asymmetry. These images also identify the location of high and low activities. These features of asymmetry and high/low activity could represent some kinds of cerebral abnormality.

According to the BEAM pictures in our experiments, we may hypothesize:

- 1). most brain diseases may cause the slow EEG activity to be increased;
- 2). the electrical activity at the location of the certain brain dysfunction might be higher than in normal subjects;
- 3). memory impairment and depression could lead to a low activity in all frequency bands between 5 and 21 Hz;
- 4). the decreased activity in some frequency bands may indicate the existence of cerebral dysfunction.

BEAM pictures not only enhance the visibility of EEGs, but also show some brain problems that unaided visual inspection of EEGs may not detect or may detect with difficulty. Thus computerized topographic mapping provides an important tool of identifying patients' brain diseases.

The system we used here and the method we developed take full advantages of modern advances in personal computers. A key feature is simplicity,

low cost, speed and ease of use. The reasons are: (1). the whole system only consists of a personal computer with an A/D converter, a tape recorder and a EEG machine (BECKMAN R511A); (2). the computing time of the data processing has been optimized. For example, it takes less than 1.5 minutes to process 10-sec 4-channel data; the mapping speed has been greatly increased so that the mapping time for a single picture is under 2 seconds. (3). the BEAM images are readily saved on a floppy disk without taking much memory and without using a large amount of polygraph paper and ink; (4). the procedure from data acquisition to final mapping is automatic, the EEG technician could use this system by simply following a few instructions, and could review a patient's BEAM images at any time by simply typing the patient's I.D. into the computer. Also, only a small investment is required to implement this system in a clinical laboratory.

The experiments described in this chapter also indicate that this system is very sensitive. A little change in some part of the brain will cause a different color distribution in that region. This sensitivity may be used for the brain study in the future.

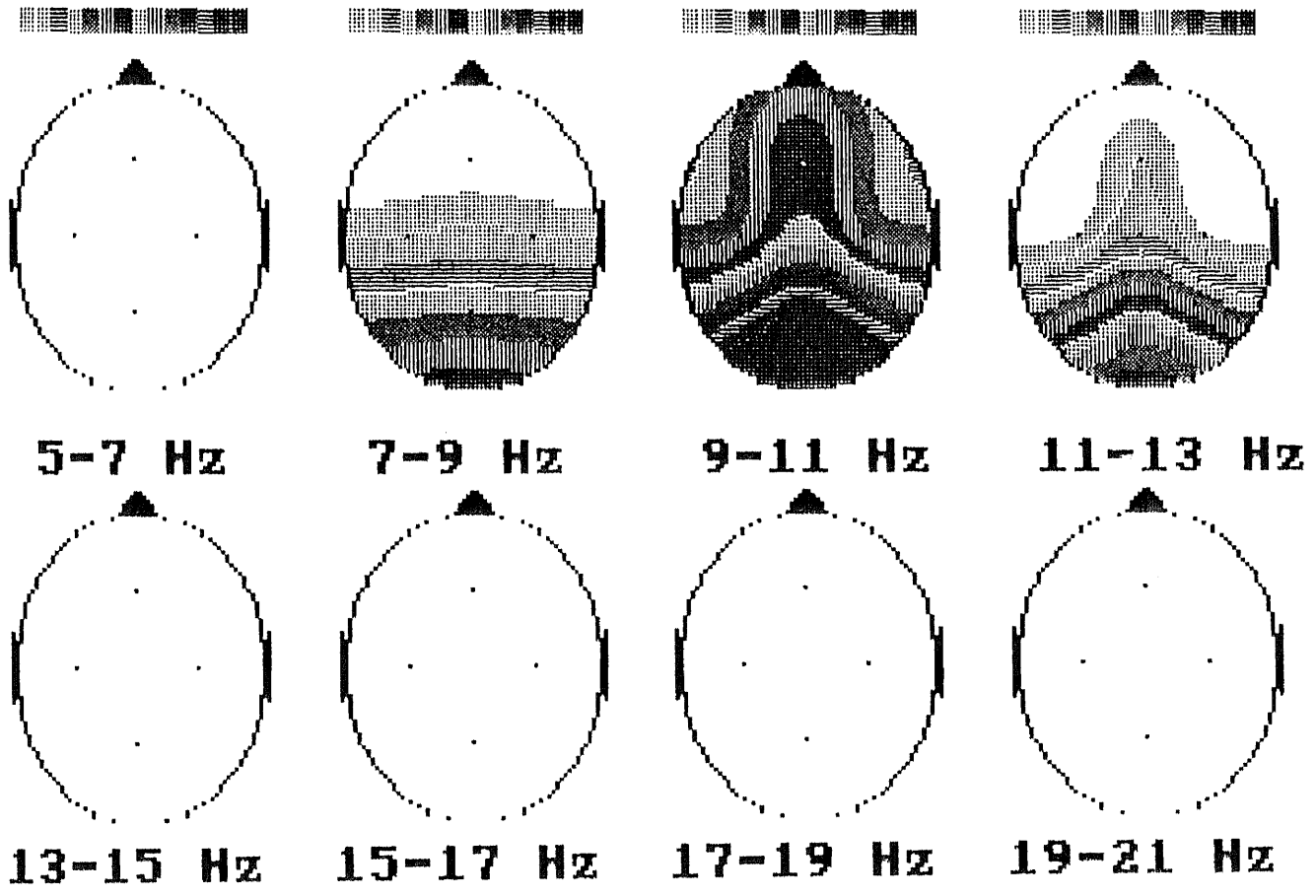


*Fig-10 Beam pictures for subject 1*

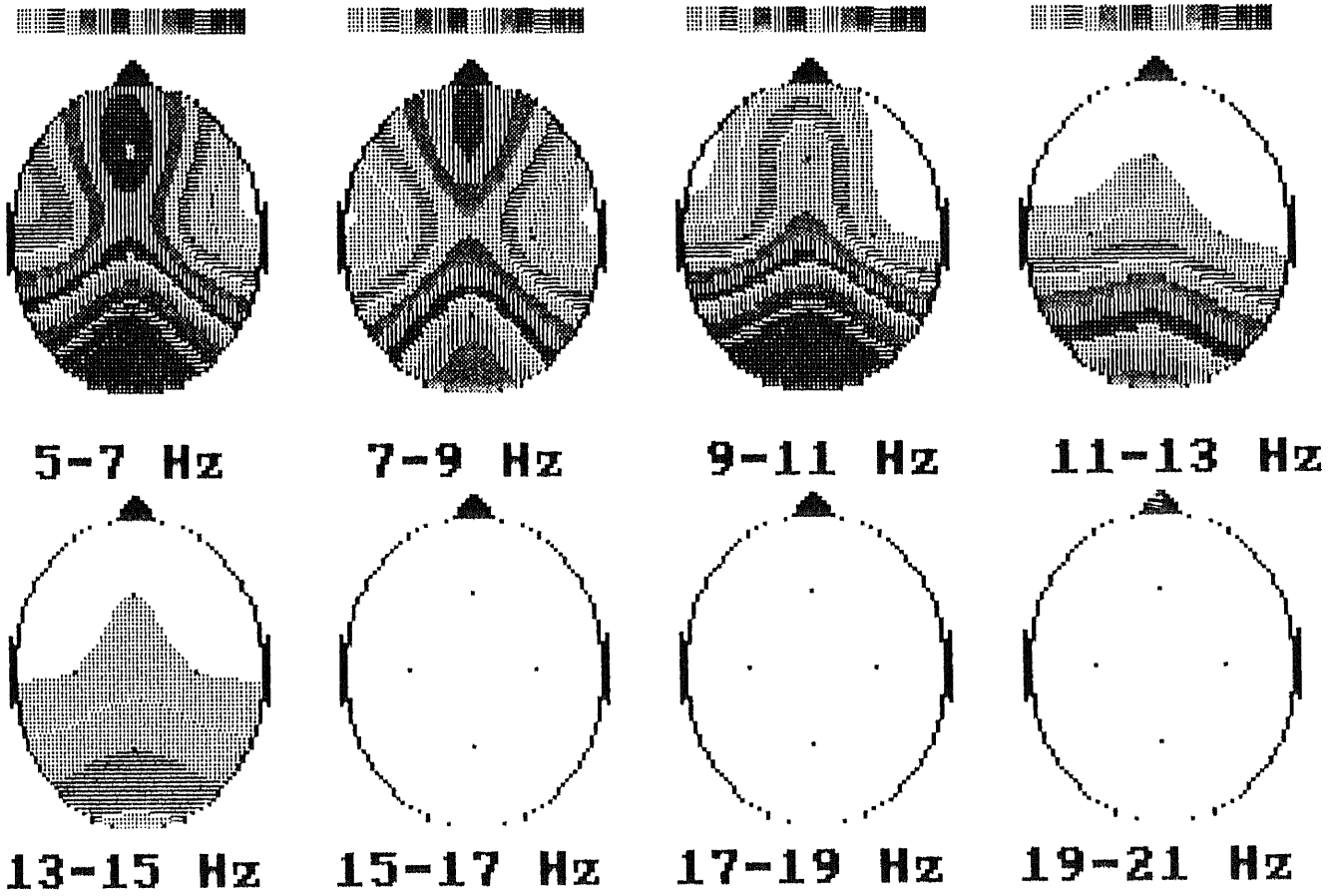


*Fig-11 Beam pictures for subject 2*

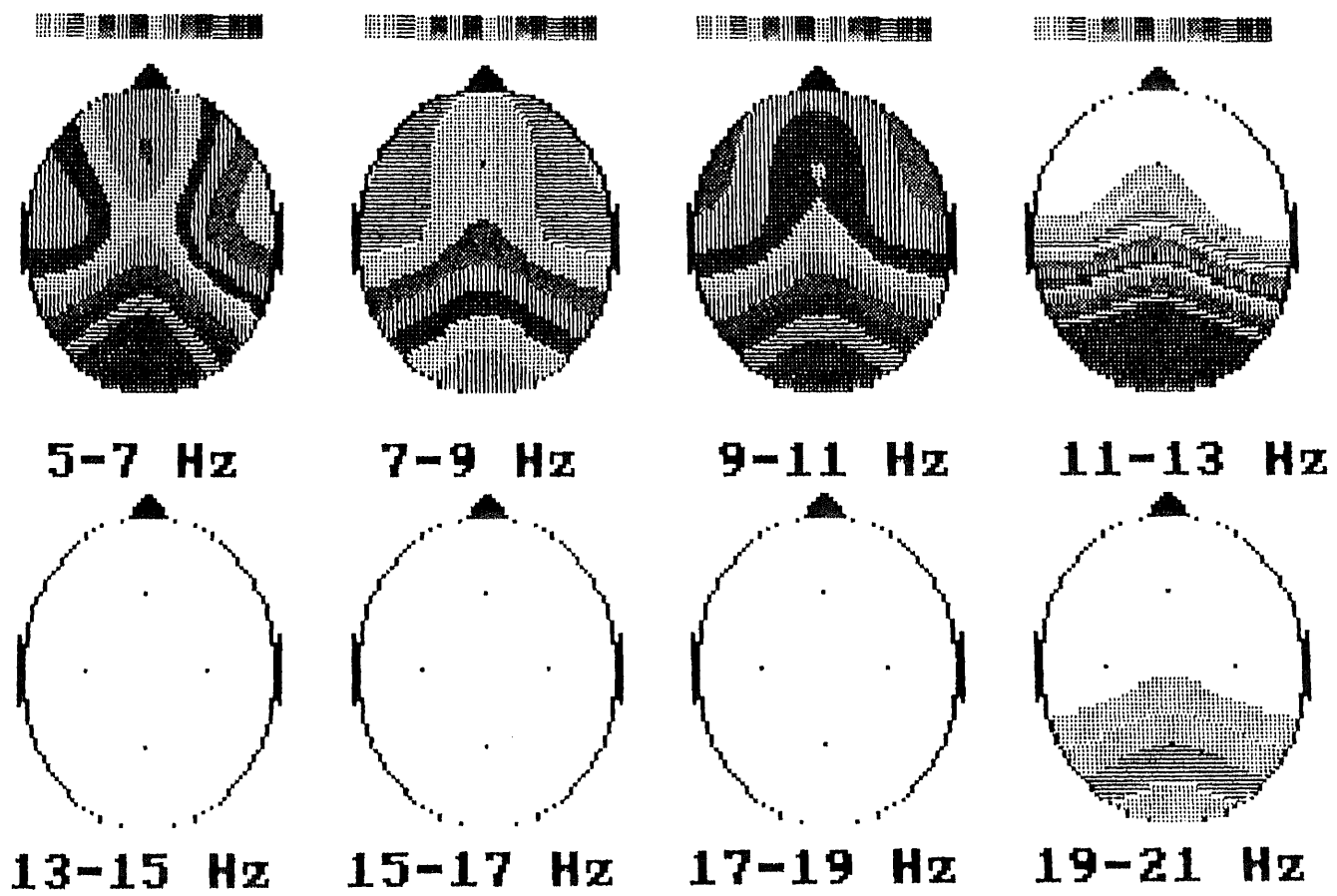


*Fig-12 Beam pictures for subject 3*

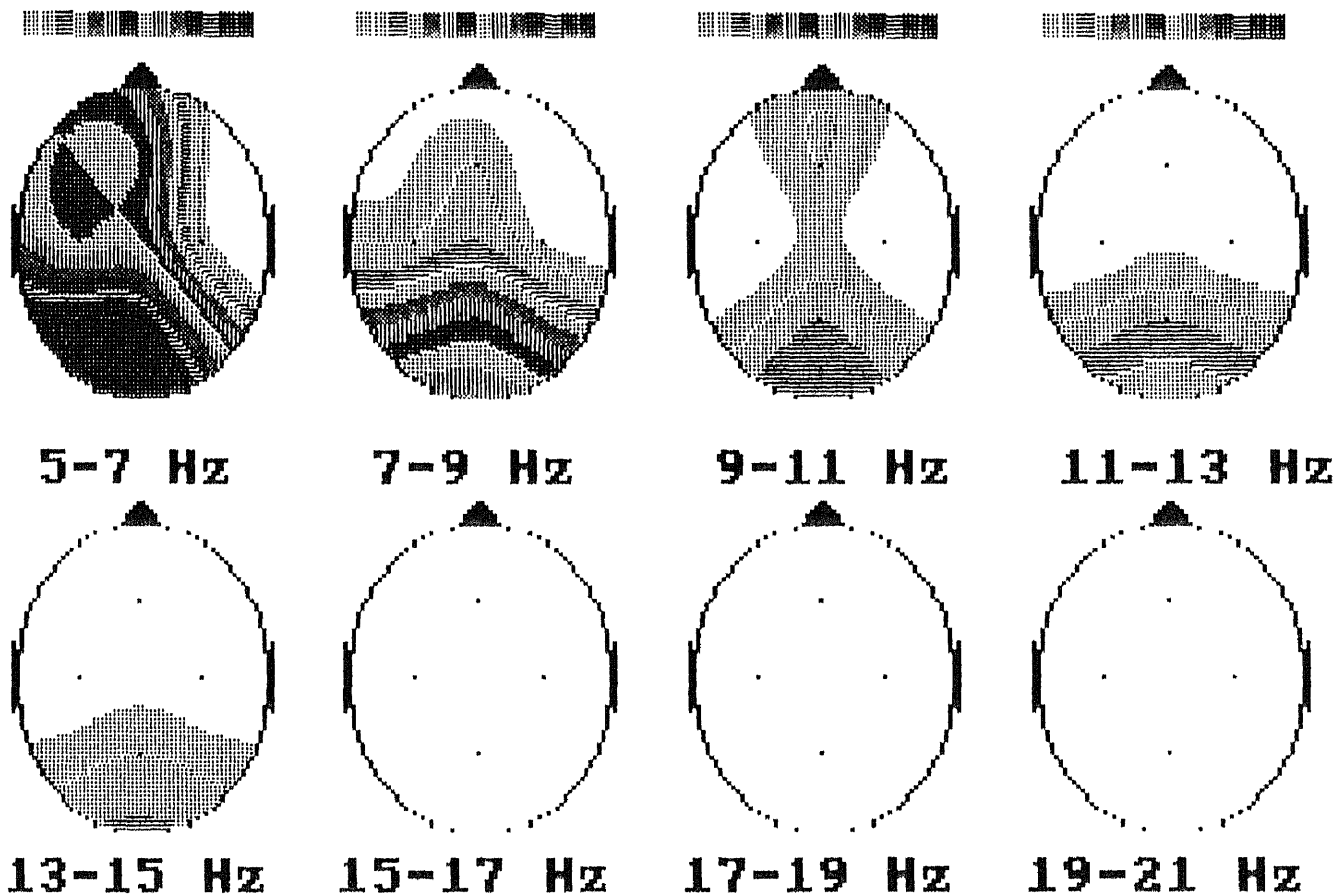


*Fig-13 Beam pictures for subject 4*



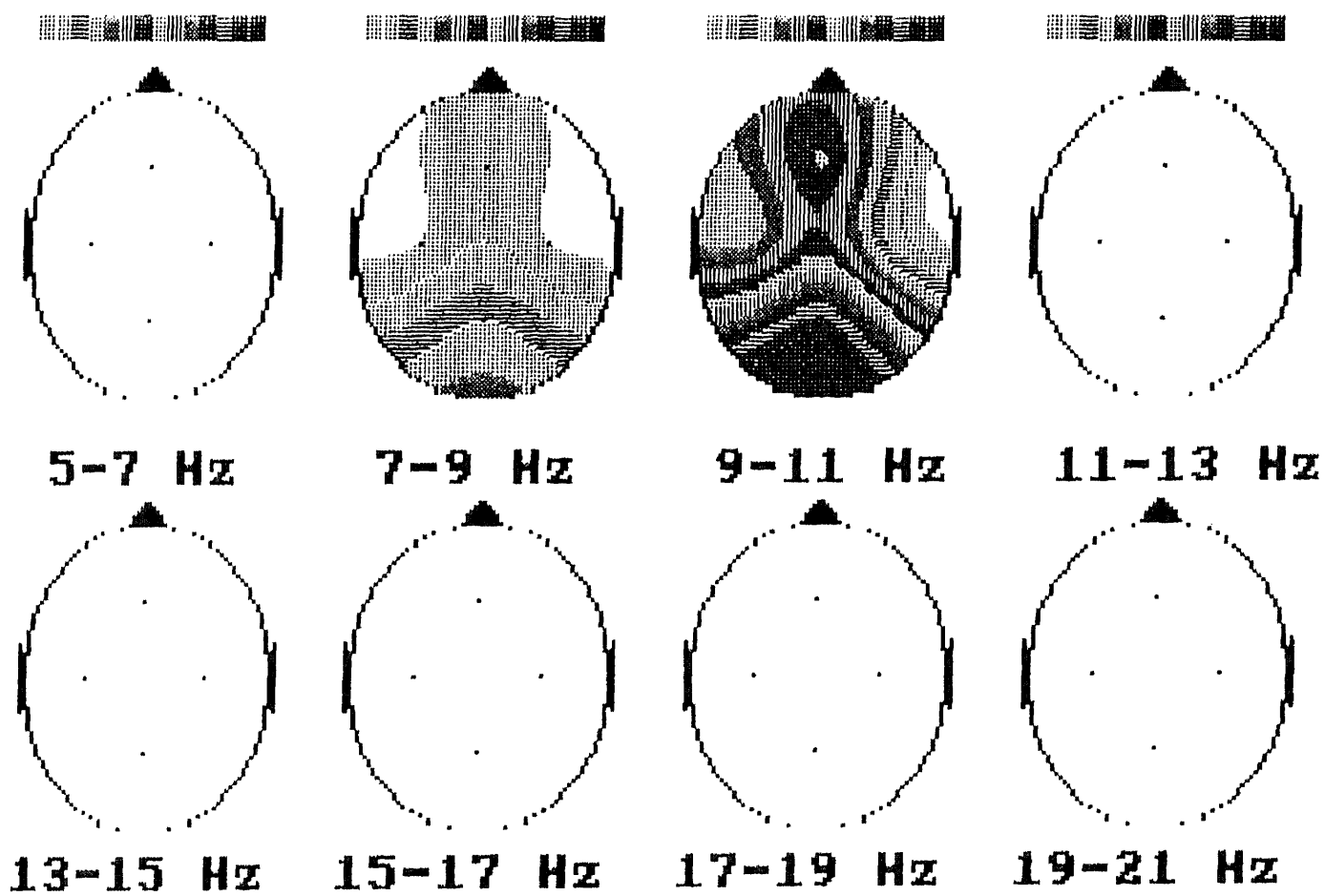


*Fig-14 Beam pictures for subject 5*

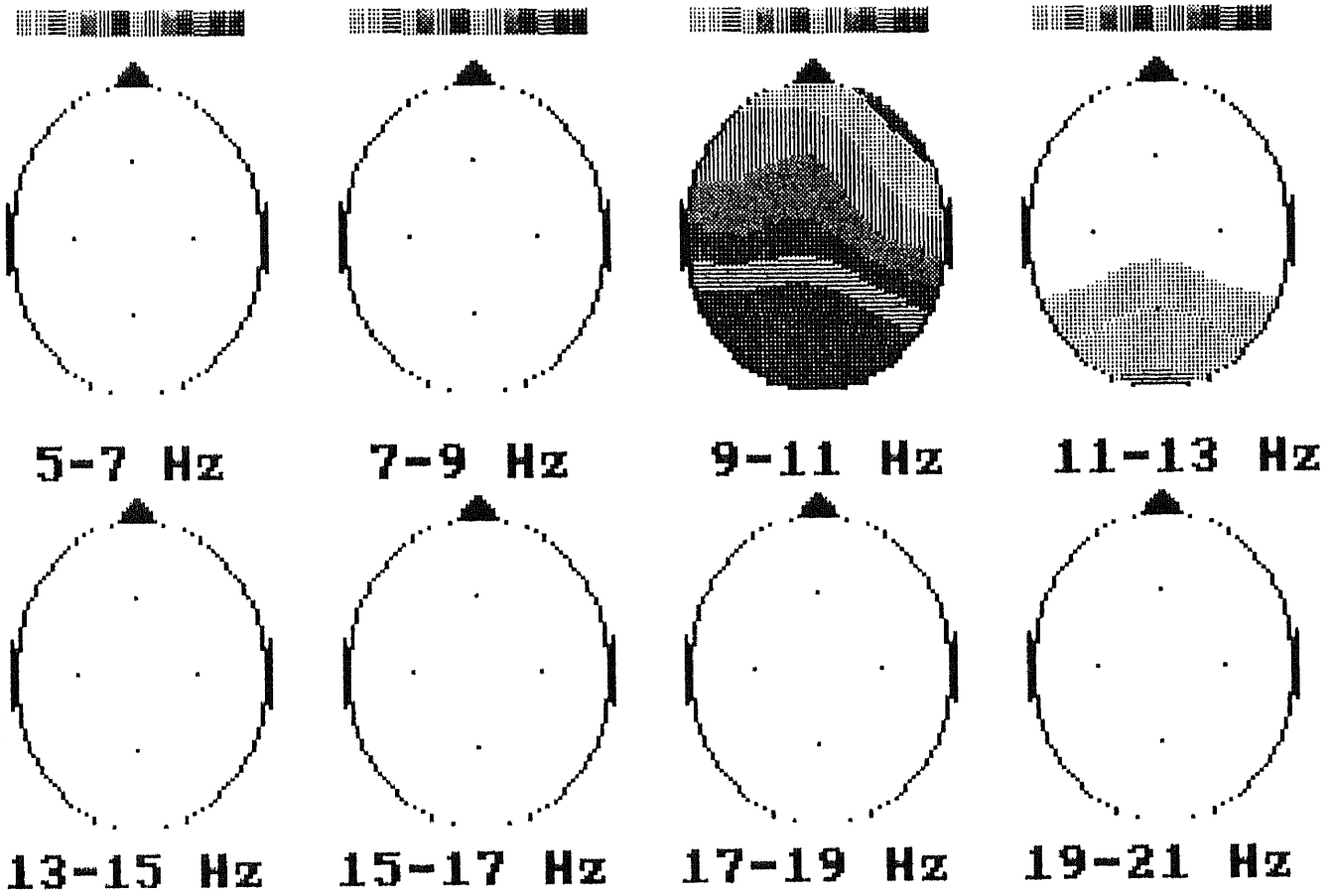


*Fig-15 Beam pictures for subject 6*

# Appendix A

## DASH-16 Hardware

### Configuration

The hardware configuration of the DASH-16 used in this project is described here.

1.) **The channel input configuration:** There are two choices, one is for *16 single ended* channels, another is *8 differential* channels. The 16 single ended configuration is used when the signal source has the same ground as the computer. For the 8 differential configuration, a signal source has one side connected to a local ground. The differential input responds to the difference between high and low input. It is used when the signal sources

have different ground with the computer.

2.)The input channel range and gain: The range and gain to be set are common to all channels, and are given in table 5

Table 5

Gain	UNIpolar	Bipolar
0.5	N/A	+/- 10. V
1	0 - 10	+/- 5.0 V
2	0 - 5	+/- 2.5 V
5	0 - 2	+/- 1.0 V
10	0 - 1	+/- 0.5 V
USER	*	*

The switch marked "GAIN, controls the full scale common to all the channels. Only one slider at a time should ever be in the "ON" position, otherwise an incorrect gain will occur. The switch "BIP and UNI" determines the ranges in unipolar or in bipolar. If the gain beyond those in Table 5 is required, it can be obtained by soldering a precision resistor into the "USER" location and selecting the "USER" position.

3.)DMA level: In practice, an A/D service routine requires checking the status or EOC of the A/D to see if the data are ready, and its execution time makes it difficult to handle data conversion rates above 10 KHz. Another serious shortcoming of a programmed transfer through the CPU is that is liable to disruption from interrupts, the time interrupt being a major culprit on the IBM PC. Thus fast A/D conversion usually takes advantage of Direct

Memory Access (DMA). In the operating DMA level, data will be transferred at the end of conversion. A switch marked "DMA" provides two DMA levels to be chosen, "1" or "3". "1" is used for a hard disk, and "3" for a floppy disk.

4.) **Base Address:** DASH-16 requires 16 consecutive address locations in I/O space. For the IBM personal computer, the reserved I/O address map is summarized as follows:

ADDRESS	DEVICE	ADDRESS	DEVICE
000-0FF	Internal I/O	378-37F	Printer
200-20F	Game I/O	380-38C	SDLC Comm.
210-217	Expansion Unit	390-399	Binary Comm.2
220-24F	Reversed	3A0-3A9	Binary Comm.1
278-27F	Reserved	3B0-3BF	Mono-disp/Printer
2F0-2F7	Reserved	3C0-3CF	Reserved
2F8-2FF	Com2:	3D0-3DF	Color Graphics
300-31F	Prototype Card	3E0-3E7	Reserved
320-32F	Hard Disk	3F0-3F7	Floppy Disk
3F8-3FF	COM1:		

To provide flexibility in avoiding conflict with IBM PC internal and peripheral devices, DASH-16's I/O address is usually set to &H300 - &H31F by the Base Address D.I.P switch.

Other choices can be made if necessary to avoid the conflict.

# Appendix B

## Index Registers of CGA Video Controller

Port 3D0 is the index register of the CGA video controller. In this project, we used the following registers:

### Index 0—horizontal line total

*Horizontal line total* determines the total number of character clock cycles per horizontal line of the display. This includes time that the beam is on for display as well as when it is off during overscan and retrace.

### Index 1—horizontal bytes displayed

*Horizontal bytes displayed* determines the actual number of character posi-

tions or bytes of the video RAM that are displayed per line. This number must be less than the horizontal total.

#### **Index 2—horizontal synchronization position**

*Horizontal synchronization position* is used to position the display horizontally. A value can be loaded between 1 and the horizontal time total. The value below 80 will lead to a part of the picture being illegible.

#### **Index 3—horizontal synchronization width**

*Horizontal synchronization width* will not produce any interesting effects. Its value depends on the monitor.

#### **Index 4—vertical lines total**

*Vertical lines total* controls the total number of lines on one full screen. Changing this register alone will not properly shrink or stretch the picture. This register has to work with Index 5 and Index 9 together to adjust the picture which is expected.

#### **Index 5—vertical adjust**

*Vertical adjust* is to adjust vertical timing parameters to be close to IEEE standard specification, that is :

$$[(Index4 + 1) \times (Index9 + 1)] + Index5 = 262$$

Where Index # is the value in register #.

#### **Index 6—vertical lines displayed**

*Vertical lines displayed* specifies the number of character rows that are actually displayed.

#### **Index 7—vertical synchronization position**

*Vertical synchronization position* is used to align the picture vertically just as the horizontal synchronization position. This value should be longer than that in the horizontal lines displayed.

#### **Index 8—interlace mode**

*Interlace mode* can be used to put the picture into different configurations with regard to interlace. There are four different modes. Among them, mode 0 and mode 2 are noninterlaced, which are usually selected as default value, and mode 1 and mode 3 are interlaced.

#### **Index 9—maximum scan line**

*Maximum scan line* determines the number of scan lines per character row and thus the maximum height of a character in text modes.



# Appendix C

## Index Registers of the EGA CRTC Controller

Port 3D4 is a CRTC index register of the EGA. In this project, we used the following registers:

**Index 0—horizontal total**

*Horizontal total* register is programmed with the number of character widths in the horizontal scan. A internal counter resets after reaching the value programmed into it. This register also controls the horizontal pixel size, a higher value producing a smaller horizontal pixel size.

### **Index 1—horizontal display end**

*Horizontal display end* register determines the number of character widths in the displayable area. After the internal counter reaches this value, the overscan begins.

### **Index 2—start horizontal blanking**

*Start horizontal blanking* register contains the count value at which the horizontal blanking signal becomes active. The right overscan ends after the internal counter reaches this value.

### **Index 3—end horizontal blanking**

*End horizontal blanking* register is programmed with the five least significant bits of the count value at which the horizontal blanking signal becomes inactive. This register also provides a skew control which delays the start of the displayable area after the horizontal total value has been reached. This allows the CRFC to access the character and attribute data, etc. If this skew is set too low, the leftmost character may appear more than once; if too high, one or more characters may disappear.

### **Index 4—start horizontal retrace**

*Start horizontal retrace* register holds the counter value at which horizontal retrace becomes active. This will initiate the beam's move to the left of the screen. This value is responsible for screen centering.

### **Index 5—end horizontal retrace**

*End horizontal retrace* register is programmed with the five least significant bits of the count value at which horizontal retrace signal becomes inactive. This register provides a retrace delay, which may be used to synchronize the retrace and blanking, etc.

### **Index 6—vertical total**

*Vertical total* register is programmed with the eight least significant bits of the vertical scan line count. The ninth bit of the vertical total is included in Index 7. An internal counter resets after reaching this value. This internal counter is the basis for vertical CRT timing.

### **Index 7—overflow**

*Overflow* register contains the most significant (*ninth*) bit of the vertical scan register. Unlike CGA, which has vertical adjust, the CRTIC on EGA is very complicated and uses the ninth bit of the vertical scan register to extend the adjust range. In this register, bit 0 is the ninth bit of the vertical total; bit 1 is the ninth bit of the vertical display end; bit 2 is the ninth bit of the start vertical blank; bit 4 is the ninth bit of the line compare. Bit 5-7 are for VGA only.

### **Index 8—preset row scan**

*Preset row scan* register determines the first displayable scan line.

**Index 9—maximum scan line**

*Maximum scan line* register contains the value of the character height.

**Index 16—vertical retrace start**

*Vertical retrace start* register is programmed with the eight least significant bits of the count value at which the vertical retrace pulse becomes active. This register initializes the beam's move to the top of the screen.

**Index 17—vertical retrace start**

*Vertical retrace start* register is programmed with the four least significant bits of the displayable area's vertical scan line count.

## References

- [1] Qian, J., Barlow, J. S. and Beddes, M. P. “*A Simplified Arithmetic Detection of EEG Sharp Transients Preliminary Results*” IEEE Trans. Biomed. Eng. Vol 35. Jan. 1988, PP11–17.
- [2] Perrin, F., Bertard, O., Pernier, J. “*Scalp Current Density Mapping: value and estimate from potential data*” IEEE Trans. Biomed. Eng. Vol BME-34, April,1987.
- [3] Desmedt, J. E., Ngvygn, Tran, H. N. and Bourguet, M. “*Bit-mapped Color Imaging of Human Evoked Potentials with Reference to the N20, P22, P27 and N30 Somatosensory Response*” Electroenceph. Clin. Neuroph. Jan. 1987, Vol 68.
- [4] Duffy, F. H., Bunchfield, J. L., and Lombroso, C. T. “*Brain Electrical activity Mapping (BEAM): a method for extending the clinical utility of EEG and evoked potential data*” Annals of Neurology, Vol 5. No.4, April 1.
- [5] Vender, A. J., Sherman, J. H. and Luciano, D. H. “*Human Physiology — the mechanisms of body function*” 4th edition, McGraw-Hill book

- company. 1985.
- [6] Brazier, Mary A.B. *"The Electrical Activity of The Nervous System"*  
3rd Ed. The Williams and Wilkins Company, 1968.
- [7] Okyere, J. G., Ktonas, P. Y. and Meyer, J. S. *"Quantification of the  
Alpha EEG Modulation and its Relation to Cerebral Flow"* IEEE Trans.  
Biomed. Eng. No.7, July,1986.
- [8] Moser, J. M. and Auton, J. I. *"Classification and Detection of Sin-  
gle Evoked Brain Potentials Using Time-frequency Amplitude Features"*  
IEEE Trans. Biomed. Eng. No.12, Dec. 1986.
- [9] Kline J. *"Biological Foundations of Biomedical Engineering"* Little,  
Brown and Company, Boston, 1976.
- [10] MetroByte *"Data Acquisition and Control — DASH-16 Manual"* Copy-  
right by MBC 1984.
- [11] Oppenheim, A. V. *"Digital Signal Processing"* Prentice-Hill, Inc. 1975.
- [12] Proakis, J. G. and Manolakis, D. G. *"Introduction to Digital Signal  
Processing"* Macmillan Publishing Company, 1988.
- [13] Norton, P. *"Inside the IBM PC"* Brady, New York,1986.

- [14] Buchsbaum, M.S., Rigal, F., Coppola, R., Cappelletti J., King C. and Johnson J. "*A New System for ray-level Surface Distribution Maps of Electrical Activity*" *Electroenceph Clini. Neurophysiol.* 1982, No.53, PP237-242.
- [15] Perrin F., Pernier, J., Bertrand, O., Giard, M. H. and Echallier, J. F. "*Mapping of Scalp Potentials by Surface Spline Interpolation*" *Electroenceph. Clin. Neurophysiol.* 1987, No.66, PP75-81.
- [16] Klierer, B. D. "*EGA/VGA — a programmer's reference guide*" 1988 McGraw-Hill book Company, N.Y.
- [17] Chasen, S. H. "*Geometric Principles and Procedures for Computer Graphic Applications*" Prentice Hill, Inc. 1978.